Synthesis of Zwitterionic Lipidoids and its Biomedical Applications

A thesis submitted by

Prudence Li

In partial fulfillment of the requirements for the degree of

Master of Science

in

Biomedical Engineering

Tufts University

August 2017

Advisor: Qiaobing Xu

Abstract

Developing drug delivery systems that can efficiently and effectively release therapeutic payload without inducing side effects has proved to be a difficult task. This is why it is becoming increasingly important to be able to synthesize tunable drug carriers where their physical and chemical properties can be specific to the targeted application. Zwitterionic lipidoids are an emerging new class of lipid-like material that have neutral charge. Many studies have cited zwitterionic lipidoids to exhibit excellent stability and low cytotoxicity due to their unique structures. As result, they play a key role in advancing drug nanotechnology. Thus, it is critical to expand the combinatorial library of synthesized zwitterionic lipidoids. By conjugating different polar heads groups with hexadecyl acrylate, new zwitterionic lipidoids were developed. Although amino acid based zwitterionic lipidoids have been studied in literature, the particular use of β-alanine as a head group has not been done. Its resulting zwitterionic lipidoid produced significantly lower cytotoxicity in comparison to current literature and makes this a novel approach to drug delivery. Their properties were then evaluated and their biomedical applications investigated.

Acknowledgements

I would like to thank my research advisor Professor Xu leading me and guiding me throughout my Master's program. Not only have I have learned so many new skills and gained a greater in-depth understanding of the biomedical field from Professor Xu, he has also pushed me to explore new topics and discover what most interests me. Thank you for advising me on my research and providing support when there were difficulties.

I would also like to thank Professor Thomas for allowing me use the chemistry department fluorimeter to conduct my CMC tests and having his students be available to assist me in any way. I would also like to thank Professor Jiang for his support and assistance whenever I needed it.

In terms of those in Professor Xu lab, I would like to thank Dr. Yamin Li for providing the lipidoid stock solutions that were used for comparison and helping me with the BA-HA synthesis. As well, thank you Zhimin Chen for assisting me with the AFM imaging of the lipidoids.

Finally, I thank all the members in Professor Xu lab. Each of you have supported me and helped in one way or another.

Table of Contents

List of Tables

List of Figures

Synthesis of Zwitterionic Lipidoids and its Biomedical Applications

Chapter 1: Introduction

1.1 Zwitterionic Materials

Zwitterionic materials are a class of materials that maintain a neutral charge, despite their high dipole moments and simultaneously possessing both highly charged cationic and anionic groups [1]. They are very commonly found in nature as osmolytes, amino acids, cell membranes, and DNA and are used by living systems to construct various tissues and provide biological responses. Recently, zwitterionic materials have taken the forefront of biocompatible materials with their super hydrophilicity and strong hydration by ionic salvation that is largely attributed by their unique chemical structures [2][3].

Zwitterionic materials have extended into many areas including surface coating of biosensors, wastewater treatment, marine coating, and carriers for proteins, drugs, and DNA.

1.1.1 Zwitterionic Surfactants

Generally, there are two types of zwitterionic groups: betaine and mixed charged pairs. Betaines are those with the same number of repeating units of positive and negative charges on a single side chain [2]. The most widely studied betaines include sulfobetaine (SB), carboxybetaine (CB), and phosphorylcholine (PC) (**Figure 1**).

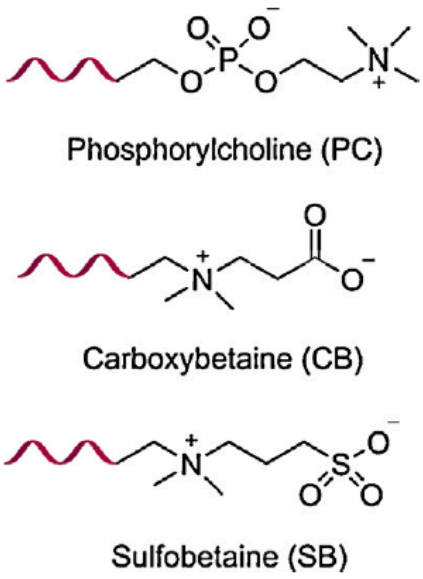

Figure 1 Chemical structures of zwitterionic molecules [3].

A key feature of PC groups is their close similarity in the chemical structures to phospholipids head group in cell membrane, resulting in reduced protein adsorption and high biocompatibility. However, due to the considerable difficulty in synthesizing, the use of PC is more limited than other zwitterionic groups. In contrast, CB is easy to functionalize and maintains that extremely low non-fouling property exhibited in many zwitterionic materials. However, SB is still the most commonly used zwitterion material due to its inexpensive nature and great potential to be commercialized. Mixed charged zwitterions are commonly amino groups and have are often pH sensitive which can be manipulated for drug delivery [2].

Zwitterionic materials have shown they possess stronger hydration than non-ionic PEG materials and are thus, often used as surfactants to coat various materials [1]. Using sum frequency generation spectroscopy, Kondo et al. investigated the interaction of water molecules with the surface of zwitterionic copolymer films. They showed that the water molecules were not strongly oriented at the zwitterionic film interface in comparison with other materials, including bare quartz, non-polymer polymer films, and positively or negatively charged polymer film. In other words, the water molecules at the zwitterionic surface are more stable and tightly bound together than at other surfaces, which then acts as a physical and energetic barrier to protein adsorption [4]. These results were consistent with the study previously conducted by He et al. that used molecular simulations to observe a lower mobility in water molecules near the zwitterionic self assembled monolayers (SAM) than that of the non-ionic tetra(ethylene glycol), as well as wider dipole orientation distributions [5].

Another example of a zwitterionic surfactant is Dioleoylphosphatidylethanolamine (DOPE), which is often used in gene and drug delivery systems. DOPE is often used as a helper lipid and formulated in combination with cationic lipids for gene delivery due to its neutral charge that allows it to destabilize the membrane at low pH and easily facilitate endolysosomal escape [6]. Studies have shown that when

used as a helper lipid, DOPE has generated higher transfection efficiencies across many cell types in comparison to another common neutral helper lipid, dioleoylphosphatidylcholine (DOPC) [7] [8]. Micelles can have a variety of structural shapes that can facilitate delivery to different degrees (**Figure 2**). Particularly with DOPE, at a low pH, its structural shape shifts into an inverted hexagonal packing structure.

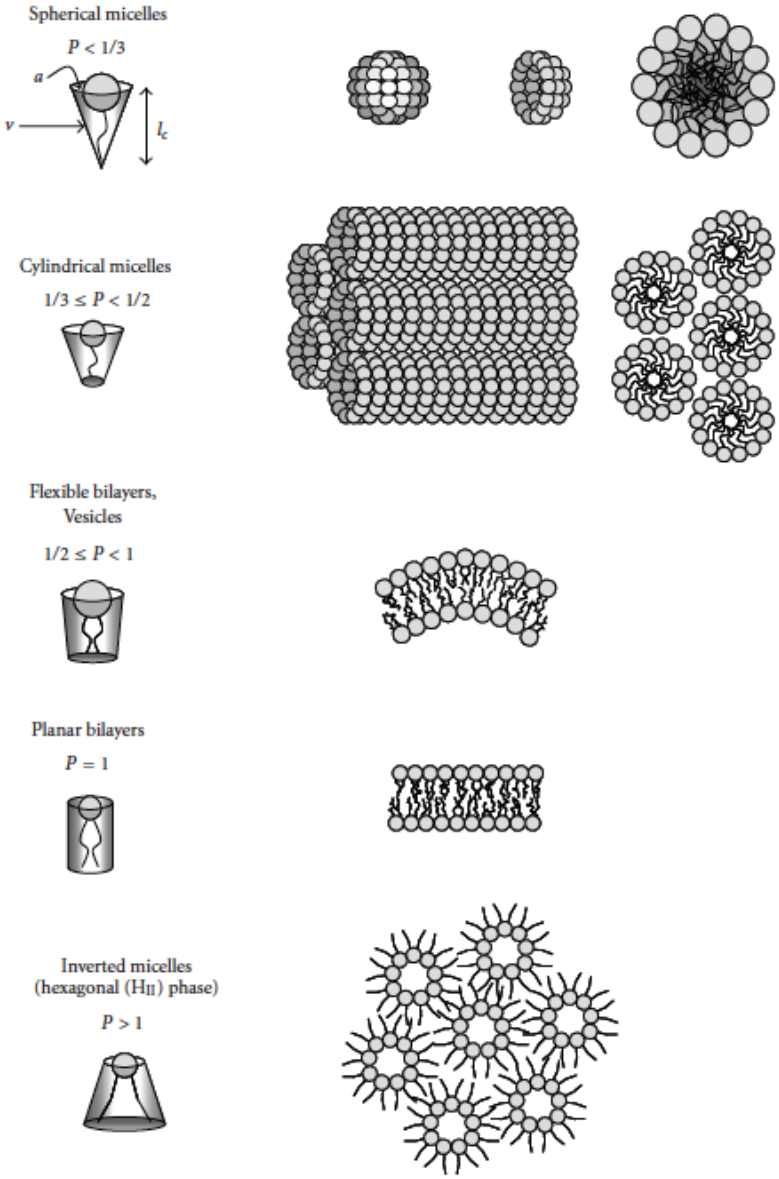

Figure 2 Different micelles structures that can be predicted using a packing parameter, P. [9].

The honeycomb like structure of the tubular structures allows electrostatic interactions to tightly condense the DNA inside the tubes. Van der Waals forces between the lipid tails surrounding the tubes then bring the tubes together. This phenomenon has been observed in many studies that have shown hexagonal structures resulting in highly efficient endosomal escape of DNA [10][11]. Other studies have also shown DOPE facilitates the release of counter ions from the positively charged lipid head group. This lower binding energy that is required means more tightly packed DNA helices can be achieved [12].

1.1.2 Zwitterionic Lipidoids for use in Biomedical Applications

Lipids have been used in biomedical applications for decades and their advantages are well known and documented thoroughly. For instance, they are highly tunable chemical, biological, and mechanical properties, protection from degradation, and show good biocompatibility [13]. Similar to lipids are lipidoids, which are a class of lipid-like structures used to facilitate cargo delivery, such as gene and protein. Zwitterionic lipioids are a particular class of neutral charged lipidoids are becoming increasingly popular. Recent studies show zwitterionic lipidoids as a very promising vehicle for cargo delivery because not only do they have good stability,

prolonged circulation in the blood, possess higher drug loading, but they are also able to reduce cytotoxicity [13]. Moreover, they are uniquely pH sensitive in a way that allows them to switch their charge and molecular conformation [13].

These unique properties that make them a very favourable candidate in biomedical applications and so, it is critical that further studies are conducted to explore their physical and chemical characteristics, as well as their potential for delivery.

Chapter 2: Objectives and Specific Aims

As the drug field continues to develop, the need for tunable drug nanocarriers that are able to efficiently and effectively release therapeutic payload becomes increasingly important. The high biocompatibility, low cytotoxicity, and low adhesion of zwiitterionic lipidoids means they will play a key role in advancing drug nanotechnology. It is for these reasons that it is critical to expand the library of synthesized zwitterionic lipidoids and to understand more about their properties and how they function. The aim of this current research: Use Michael's addition to synthesize zwitterionic lipidoids and evaluate their properties, and to investigate their biomedical applications.

As previously stated, many studies have cited amino acid based zwitterionic lipidoids to exhibit excellent stability and low cytotoxicity due to their unique structures. As a result, the study focused on synthesizing amino acid based zwitterionic lipidoids. The study consisted four components: chemical characterization via a series of tests including thin layer chromatography (TLC), flash chromatography, and nuclear magnetic resonance spectroscopy (NMR) to confirm the zwitterionic lipidoid structure, physical characterization of its morphology and study of its self assembly behaviour, a biocompatibility study investigating its cytotoxicity, and examining its efficiency as a drug carrier using Doxorubicin as a model. The self-assembly behaviour of the lipidoid was assessed by

analyzing their critical micelle concentration (CMC), which indicates the tendency of self-assembly in aqueous solution. This study used the Pyrene 1:3 ratio method to determine the CMC and was measured using a florescence spectrophotometer. The morphology of the micelles was then observed using atomic force microscopy (AFM). The results from the study were compared with currently existing lipidoids in the Xu combinatorial lipidoid library.

Chapter 3: Synthesis of Zwitterionic Lipidoid

3.1 Introduction

3.1.1 Current Lipidoid Library

Recently, combinatorial synthesis of these lipidoid nanoparticles has emerged as a means to synthesize large libraries of up to more than 100,000 molecules more efficiently for the development of delivery vehicles. High-throughput screening can then be used to evaluate and identify the top performing lipid structures for delivery of a particular cargo and tailor their physical and chemical properties for a specific medical application.

Many types of synthesis methods can be used to develop lipid combinatorial libraries, such as solid-phase synthesis, epoxide-amine addition, thiol-yne click chemistry, alkylation addition of amines, and Michael's addition reaction [14].

Over the last several years, the application of Michael's addition chemistry in the development lipid-like materials has been gaining traction, despite being widely used in organic synthesis for more than 125 years [15]. Michael addition is a one-step process conjugation addition reaction that requires no additional solvents or catalysis, where the α, β unsaturated carbonyl is on a hydrocarbon tail and the amine group is on a head [14].

The first combinatorial library synthesized by Michael's addition conjugated the amine groups with three types of alkyl chains (acrylamide, acrylate, and epoxide). Sun et al. synthesized these lipidoids and tailored their characteristics for purpose of DNA delivery [16]. Using these modified lipidoids, Wang et al. expanded on the library by functionalizing the lipidioids with varying degree of saturated alkyl chains, as well as producing bioreduicible lipidoids, characterized by the presence of a disulfide bond (**Figure 3)** [17][18].

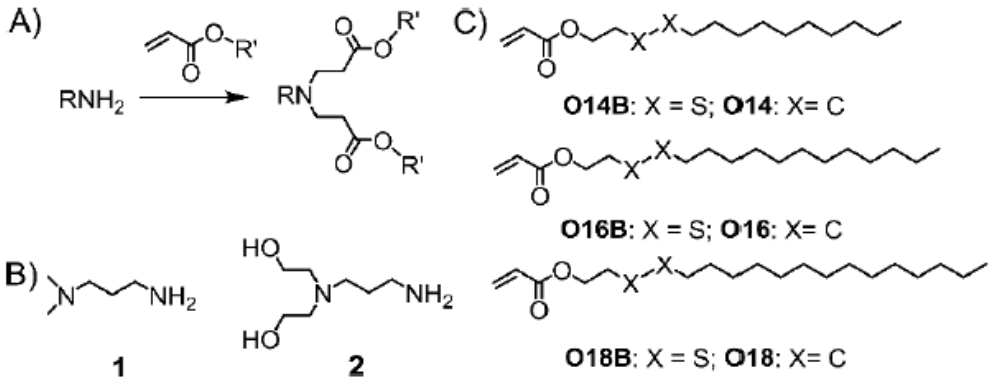

Figure 3 Combinatorial library of bioreduicible lipidoids [20]

Many of these synthesized lipidoids have been evaluated for their suitability in gene and protein delivery and have shown to be good candidates for transporting gene and proteins into the cells [18-21]. Particularly, Wang et al. investigated the effects of tail saturation on delivery efficacy of DNA or mRNA using the saturated alkyl chain

combinatorial library and has shown lowered delivery efficacy with increasing tail saturation [18].

3.1.2 Zwitterionic Lipidoid

Similar to the current lipidoid library, the zwitterionic lipidoids were synthesized through Michael's addition. Specifically in this study, the acrylate used was hexadecyl acrylate and was conjugated with a series of different head groups, including β-alanine, 5-aminovaleric acid, taurine, and O-phosphorylethanolamine (**Figure 4**).

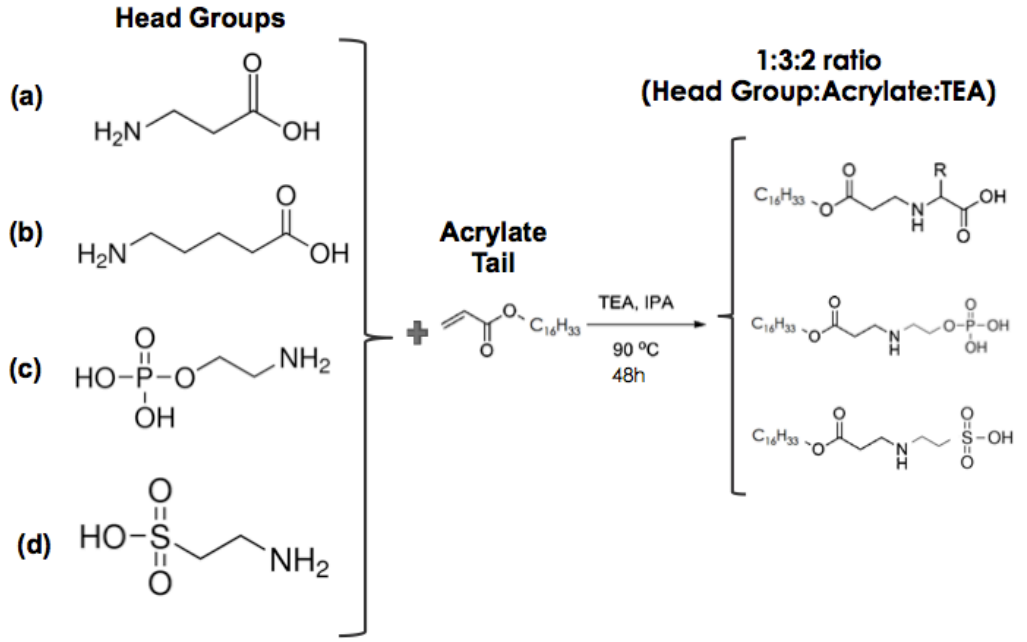

Figure 4 Synthesis of Zwitterionic lipidoids using Michael's addition with Hexadecyl acrylate tail and amino acid heads, including a) β-alanine, b) 5-aminovaleric acid, c) O-phosphorylethanolamine, and d) taurine. TEA and IPA was added to the mixture and was stirred at 90°C for 48 h.

The synthesis of these zwitterionic lipidoids followed the same procedure as the one outlined by Dong et al [22]. Briefly, the synthesis involved mixing the acrylate and amino acid with TEA at a 1:3:2 molar ratio of Head group:acrylate:triethylamine, as well as IPA, and then was stirred for 48 h at 90°C with a stirrer bar.

3.1.3 Tools for Chemical Characterization

3.1.3.1 Thin Layer Chromatography (TLC)

Thin layer chromatography (TLC) is a technique that is generally used to separate non-volatile materials. Particularly for this study, TLC was used to determine the mobile phase necessary to purify the lipidoid product and confirm the synthesis of the product.

3.1.3.2 Flash Chromatography

Flash chromatography is a separation technique that is used to purify products and relies on the difference in partitioning behaviour between a mobile phase and a stationary phase. The compound being separated interacts with the stationary phase by charge, relative solubility, or adsorption. In this particular study, the stationary phase used was a silica gel column, which is a slightly acidic medium that provides good separation. The mobile phase is used as an eluent and is pushed through

a short column, containing packed adsorbent, under gas pressure. The purified product then gets ejected into glass vials.

3.1.3.3 Nuclear Magnetic Resonance (NMR)

Nuclear magnetic resonance (NMR) is a high-resolution spectroscopy to determine the physical and chemical components of atoms and molecules that make up a sample. In this study it will be used to confirm the structural identity of the zwitterionic lipidoid. NMR uses a magnetic field to generate spinning charges which then measures the energy differences to determine structural properties.

3.2 Approach to Synthesis

3.2.1 Materials and Methods

All amino acids used in the synthesis of the zwitterionic lipidoids, including β-alanine (BA), 5-aminovaleric acid (5A), taurine (T), and O-phosphorylethanolamine (OPA) amine were purchased from Sigma-Aldrich (St. Louis, MO). For convenience, all zwitterioninc lipidoids will be referred to by an acronym denoting the amino acid and acrylate used: BA-HA, 5A-HA, T-HA, OPA-HA, with the first set of letters signifying the amino acid and the latter being the acrylate (hexadecyl acrylate). Each amino acid was mixed with hexadecyl acrylate, and triethylamine (TEA) at a 1:3:2

molar ratio, and then dissolved in 0.5-1mL of isopropyl alcohol (IPA), all of which were purchased from Sigma-Aldrich (St. Louis, MO). The solution was then stirred on a stirring plate at 90°C for 48 hours.

TLC was used to determine the mobile phase required to purify the product. The mobile phase used was a mixture of dichloromethane (DCM) and methanol (MeOH). Various mobile phase solutions were tested to find the most appropriate ratio of DCM:MeOH ratio, including 1:1, 4:1 and 10:1. DCM and methanol used were purchased from Sigma-Aldrich (St. Louis, MO). Once the most appropriate mobile phase was determined, the zwitterionic lipid product was purified by flash chromatography and TLC was conducted again to verify the product. The organic solvent was then removed by rotary evaporator and placed in a vacuum overnight. The zwitterionic lipidoid structure was confirmed by NMR.

All lipidoids from the current lipidoid library used in this study was prepared by Dr. Yamin Li from Dr.Xu laboratory at Tufts University. The synthesis reaction involves using Michael's addition to conjugate amine to alkyl chains (**Figure 5**). Two lipidoids from the current Xu library were used to compare against the zwitterionic lipidoids, including 80-O16B and 87-O16B. The nomenclature of these lipidoids is as follows: 80 detnoes the head group, 16 is the number of carbons in the hydrophobic tail of the

acrylate, and B signifies it as a bioreducible lipidoid, evident by the disulphide bond in the hydrophobic acrylate tail.

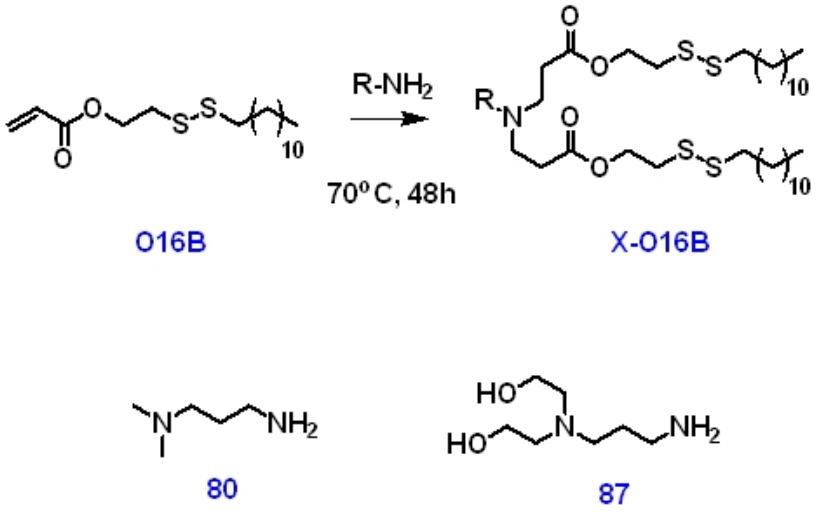

Figure 5 Synthesis reaction of the current lipidoid library that Zwitterionic lipidoid BA-HA will be compared against.

3.2.2 Chemical Characterization of Zwitterionic Lipidoids

Due their super-hydrophilic nature, amino acid based zwitterions are insoluble in most organic solvents and so, it is very difficult to dissolve zwitterionic lipidoid products [3]. This means that even having synthesized the lipidoid products, they cannot be purified and used. As a result, despite having intended the zwitterionic lipidoid library to comprise of four lipidoids, only two were successfully synthesized and purified for use. Furthermore, due to time constraints, the study will only focus on one zwitterionic lipidoid. Of the four amino acids that were used, BA and 5-A were dissolved in DCM for purification and successfully synthesized and verified by NMR. The lipidoid products made with the remaining two amino

acids, taurine and OPA, were unable to dissolve in any of the organic solvents that were tested, including DCM, methanol, ethanol, chloroform, acetonitrile, acetone, and DMSO. The problem is that the lipid head is very polar and thus requires a very polar solvent to dissolve it. However the lipid tail is extremely non-polar and as a result, when solvents such as DCM and methanol are used, only the lipid head is dissolved while the tail does not.

BA and 5-A were successfully dissolved in DCM and purified using TLC and flash chromatography. The plates used in TLC are coated with a thin layer of a substance, called an absorbent. The absorbent acts as a stationary phase that provides a surface that allows the solution to adhere to, which in the case of this study was silica gel. The lipidoid was dissolved in an organic solvent, such as DCM, and a single drop was added onto the bottom of the TLC plate. It was then placed in the mobile phase until the mobile phase reached near the top of the slide. Ninhydrin was then used to stain the product and causes a red/purple colour change that allows us to observe the reaction.

The basis of TLC is that the solute and the mobile phase compete for binding places on the stationary phase. The mobile phase for TLC is often a combination of different organic solvents including, Ultra B (mixture of DCM, ammonia, and methanol) and either DCM, acetyl acetate, or

methanol. For the purpose of this study, we used a mobile phase with DCM:MeOH. Ammonia was removed from the Ultra B as it is usually used to deprotonate the base. However, if used, the ammonium would also deprotonate the carboxylic acid in the reaction due to its high polarity.

Since silica gel is polar, the more polar compound of the two will have a stronger interaction with the it and is able to displace the mobile phase from the binding places. Consequently, the less polar compound travels further up across the plate and results in a higher retention factor, or R_f. The R_f value is the ratio of the distance travelled by the compound and the distance travelled by the solvent (**Figure 6**).

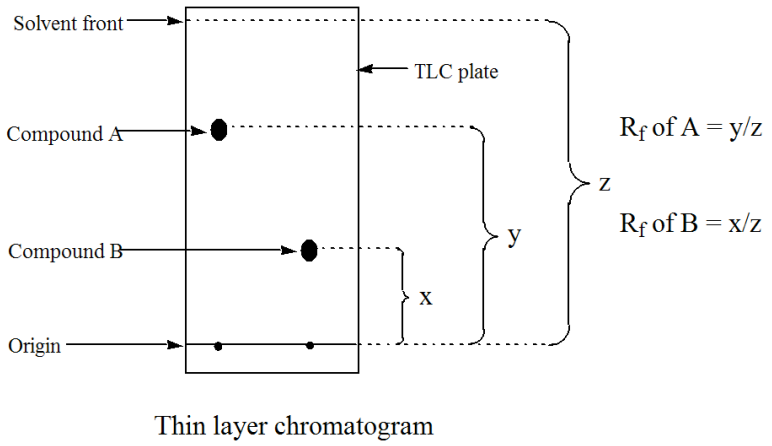

Figure 6 Thin Layer Chromatography (TLC) [23].

By adjusting the ratio of DCM:MeOH in the mobile phase, the distance the product travels across the plate can be fixed to achieve an R_f value of 0.3-0.4. For instance, an increase in DCM in the mobile phase will cause the mixture to be less polar and thus, less capable of displacing solutes from

the silica binding places. As a result, the product will not travel as far on the plate. Various DCM:MeOH were tested including 1:1, 4:1, and 10:1. A mobile phase with a 10:1 DCM:MeOH ratio was determined to be the most appropriate for the purification of the product. This mobile phase also allowed us to confirm the reaction had occurred and the products, BA-HA and 5A-HA, had formed (**Figure 7**).

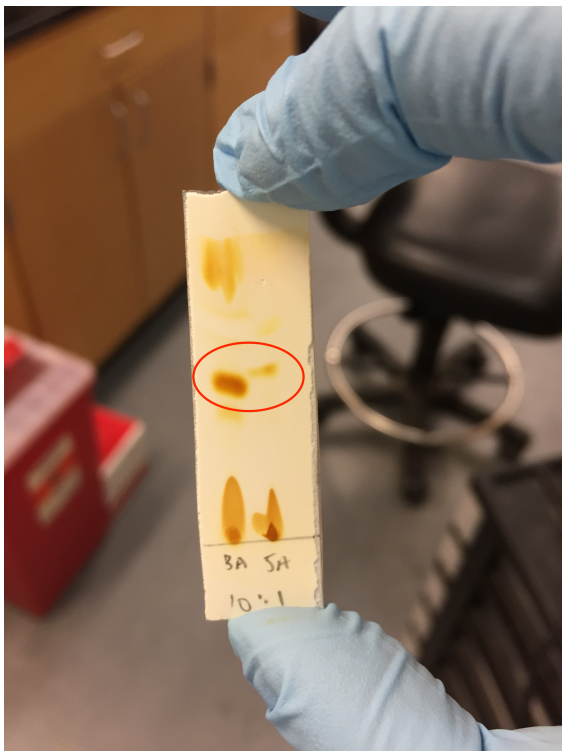

Figure 7 TLC of the BA-HA and 5A-HA lipidoid product using a 10:1 DCM/MeOH mobile phase. R_f value is in ideal range indicating the product, indicated in the red circle, has been properly synthesized. Other spots on the glass slide are impurities.

After synthesizing the products, their structures were verified using proton NMR (**Figure 8** and **Figure 9**). Each chemical group has its own peak. The peaks are integrated to give relative intensities. When these values are compared with the proton estimation generated by the program, the structures can be confirmed.

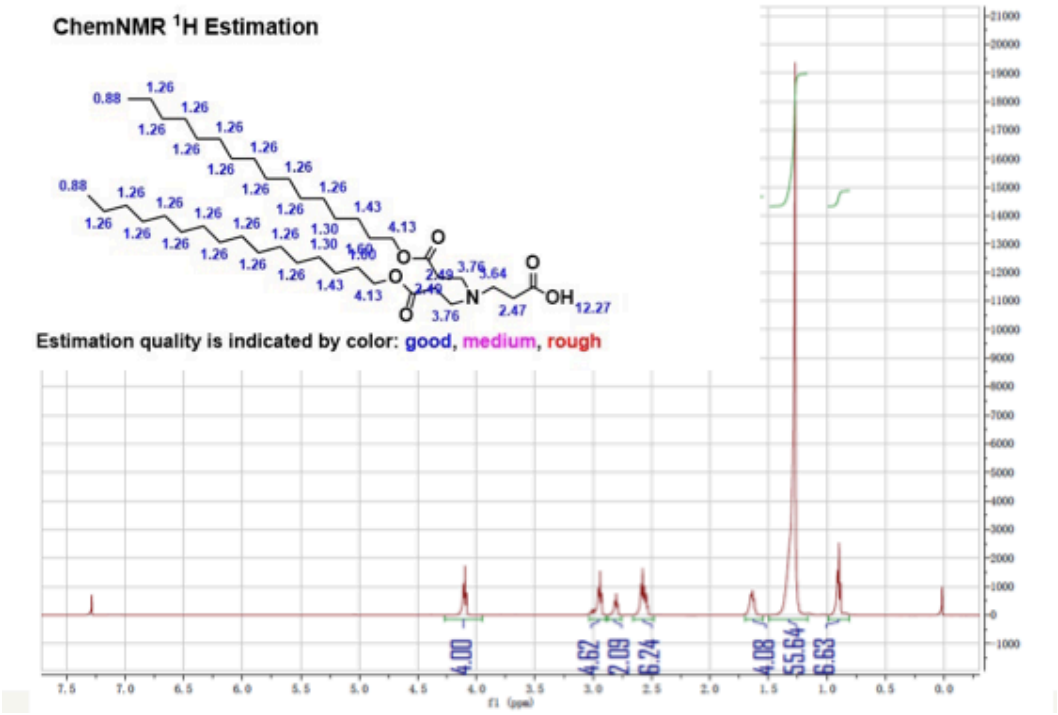

Figure 8 Proton NMR graphs and their respective proton estimations generated that confirm the structure of the zwitterionic lipioid, BA-HA.

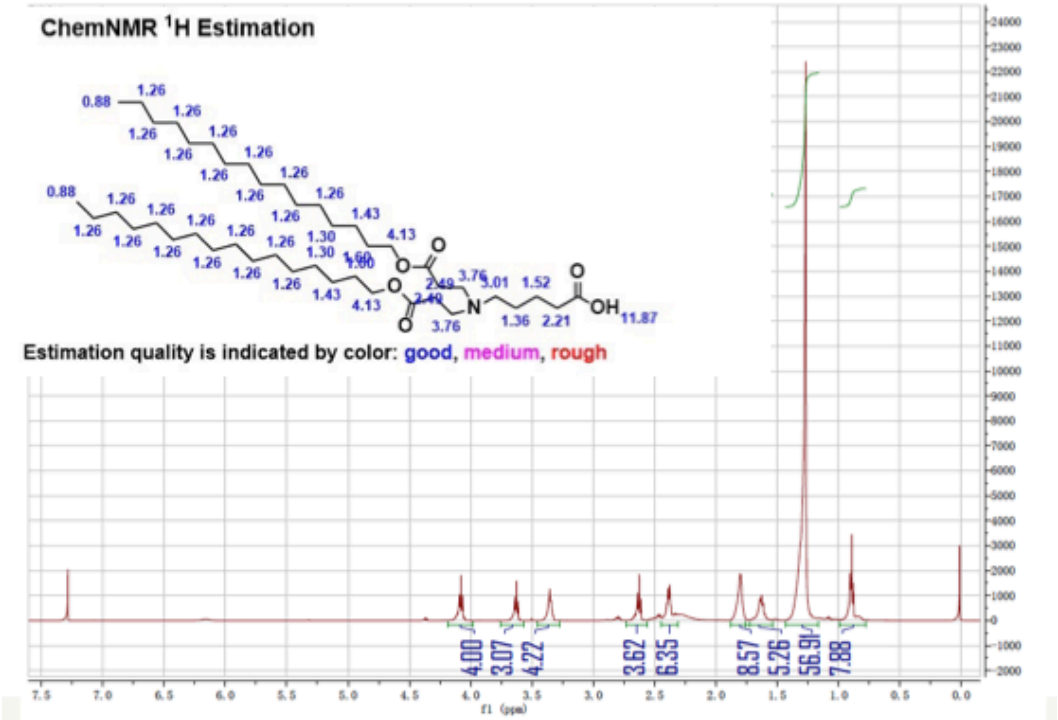

Figure 9 Proton NMR graphs and their respective proton estimations generated that confirm the structure of the zwitterionic lipioid, BA-HA.

Chapter 4: Physical Characterization of Zwitterionic Lipidoid and Comparison with Other Lipidoids

4.1 Introduction

4.1.1 Critical Micelle Concentration (CMC)

Critical micelle concentration (CMC) is the minimum concentration of the surfactants that is required for micelles to form and allows for additional surfactants to be encapsulated within. CMC is dependent on a variety of separation conditions including buffer pH, temperature, addition of organic modifers or electrolytes, additives, or ionic strength of the aqueous solution [24]. Lipidoids are critical delivery vehicles that contain the therapeutic payload. Thus, it is essential that the surfactants can form the micelles in the transportation medium and that it can be proven conclusively. Measuring the CMC value allows us to confirm this.

4.1.3.1 Conventional Methods

Typically, CMC can be measured using a number of methods including using spectrophotometry, electrical conductivity, surface tension, or light scattering [25]. Many of them have their drawbacks, however, as they are not sufficiently sensitive to be able to measure the CMC if its value is very low and may only be able to provide a very large range of CMC values, such as is the case with the light scattering method [26][27]. As well, certain electrophoresis methods use indicator dyes, which are infused into the micelles and in fact can alter the cmc value [25]. In contrast, the use of

pyrene fluorescent is much more sensitive to subtle changes in CMC even at low values [27].

4.1.3.2 Pyrene 1:3 Ratio Method

CMC can be determined using the 1:3 Pyrene Method which utilizes the poor solubility property of pyrene in water to observe the distribution of pyrene crystals surrounding at 370-400 nm [28]. The 1:3 ratio refers to the ratio of the first vibronic peak to the third vibronic peak. The intensity of the peaks is directly proportional to the polarity of the environment. For instance, a high 1:3 ratio occurs when the surfactant concentration in the solution is less than its CMC value. Since no micelles are formed, the pyrene crystals are distributed in solution surrounded by highly polar water molecules. In contrast, when the surfactant concentration is greater than its CMC value, there is a low 1:3 ratio. As a result, micelles form surrounding the pyrene crystals, which have a lower polarity than the water molecules. The changes in the 1:3 ratio as a function of surfactant concentration can be modeled using the Sigmoidal Equation, where y represents the 1:3 ratio of pyrene, A_1 is the upper constant in 1:3 ratio curve, A_2 is the lower constant in 1:3 ratio curve, x is the concentration of surfactant, x_0 is the centre of sigmoid, and Δx is the difference in concentration of samples.

$$Y = \frac{A_1 - A_2}{1 + e^{\frac{x - x_0}{\Delta x}}} + A_2 \qquad (1)$$

4.1.2 Particle Size Measured Using Dynamic Light Scattering (DLS)

4.1.4.1 Techniques for Measuring Particle Size

There are many techniques for measuring particle size and particle size distributions, some of which include electron microscopy, static light scattering (SLS), Raman correlation spectroscopy, fluorescence correlation spectroscopy, forced Rayleigh scattering. However, these techniques have their disadvantages. For instance, electron microscopy involves drying the sample and then using imaging methods to measure the size. The problem is that the nature of the species in liquid dispersion is very sensitive and can be altered when drying the sample or placing it on a surface [29]. As a result, the measurements taken can be inaccurate. Another technique for measuring particle sizes is dynamic light scattering (DLS). It is a widely used technique that is classified as hydrodynamic and is able to determine particle size and particle size distribution of small particles in suspension. In other words, hydrodynamic quantities, such as translational and rotation diffusion coefficients, are directly measured and uses theoretical relations to determine the corresponding shapes and sizes [29]. DLS is incredibly versatile and easy to use. Any suitable suspending liquid can be used with no calibration required. The same cannot be said for other particle sizing techniques such as SLS and microscopic analyses [29]. DLS only requires seconds to minutes to be quantified measurements. As well, DLS can measure particle sizes as

small as a single nanometer in diameter [29][30]. Due to its precision and ease of use, DLS will be used to measure particle sizes for all lipidoid samples in this study.

4.1.4.2 Dynamic Light Scattering (DLS)

DLS was initially developed not with intention of measuring particle sizes, but to inspect the alignment of a light scattering system in 1972. Seven years later, the first size measurements were taken and began to gain wide acceptance among experts throughout the next decade [31]. DLS works on the basis of Rayleigh scattering that states light scatters uniformly in all direction when particles are smaller than incoming wavelength. The particles are suspended in liquid and thus undergo Brownian motion and so, the distance between them is constantly changing. This means the intensity of the scattered light will fluctuate with time. DLS uses a laser beam that is directed through a polarizer and into the sample, which then scatters through another polarizer and is detected. The system then analyzes the fluctuations in scattering intensity as a function of time and uses the known viscosity of the medium to determine the diffusion coefficient of the particles [31]. The parameters allow particle diameters to be calculated from the data.

4.2 Materials and Methods

4.2.1 AFM

Stock solution of the lipidoids was prepared at 1 mg/mL in phosphate buffered saline (PBS) that was purchased from Sigma Aldrich (St. Louis, MO). This is particularly important because the purpose of the atomic force microscope (AFM) imaging is to observe the morphology of the micelles formed by the lipidoid molecules, which will only occur if the lipidoid concentration is greater than the CMC value.

The samples were prepared on silica wafers prior to AFM imaging. First, the wafers were cleaned by sonicating them in 100% ethanol and then by DI water for 5 minutes each. The silica wafers were then quickly dipped in the lipidoid stock solution. The samples on the wafers were left to air-dry for several hours. Once dry, the wafers were washed with DI water to remove any salts from the PBS and left to air-dry overnight. AFM measurements were then taken using these samples.

Lipidoid samples were measured by AFM (Dimension^{TM} 3100, Veeco, Lowell, MA) using the tapping mode and its corresponding configurations with the Nanoscope 730 software. The probe with the cantilever placed on top was loaded onto the AFM system such that the probe is parallel to the groves along the support. The position of the camera was adjusted so that the tip is in the middle of the camera. The laser was then adjusted so that

it diffracted off the tip of the cantilever. The system was synchronized with the computer by manually adjusting the red dot to the centre of the grid using the knobs. The silica wafer was then transferred to the stage of the AFM system. Once the tip and surface of the instrument was located, the cantilever was auto-tuned and the configurations and parameters were set with the scanning mode set as tapping mode.

4.2.2 CMC

Pyrene and pure ethanol were purchased from Sigma Aldrich (St. Louis, MO) and used to prepare a stock solution of 4mM pyrene in 100% pure ethanol and then diluted in ethanol at 1:10 dilution ratio to achieve a final concentration of 400μM. The pyrene solution was then further diluted with DI water at a 1:5 dilution ratio to obtained a final pyrene concentration of 80μM. It should be noted that the pyrene in ethanol solution was diluted with ethanol and DI water only immediately prior to preparing the samples for measurement. This was done to avoid precipitation of pyrene in the water solution, which may cause errors in fluorescent excitation. To prevent interference of ethanol to the polarity of the solution environment, the concentration of ethanol was maintained at a 0.5% v/v, which has been cited to have no effects on the measurements [32]. 50uL of 80 μM pyrene was added to determined amounts of carrier (either lipid or polymer) stock solutions and DI water to obtain a final sample volume of 2mL. Carrier stock solutions were prepared in water at 1mg/mL. The

solution was sonicated until the mixture was homogenous or evenly dispersed. After sonication, the sample was transferred into a UV cuvette and measured using a fluorimeter. The excitation and emission spectra were measured using the parameters cited in **Table 1**

Table 1 Fluorimeter parameters for measuring excitation and emission spectra to measure CMC.

	Emission Spectra	**Excitation Spectra**
Excitation Wavelength (nm)	335	250-390
Emission Wavelength (nm)	350-550	400
Excitation Slit (nm)	2.5	2.5
Emission Slit (nm)	2.5	2.5
Step Size (nm)	1	1
Integration Interval (s)	0.3	0.3

4.2.3 Particle Size

Lipidoid stock solutions at 1 mg/mL were prepared in PBS and then diluted with DI water at 1:100 dilution ratio. The particle sizes were then measured by DLS. The particle sizes were then measured by DLS using a zeta potential machine and the BIC Particle Solutions software.

4.3 Results and Discussion

4.3.1 AFM

AFM is a widely used high-resolution microscopy technique that can be used to determine the morphology of micelles. AFM imaging of the lipidoids can provide greater understanding of the self-assembly behaviour of lipidoids and their structure. **Figure 10** shows micelles formed by BA-HA, 87-O16B, and 80-O16B at a 1 mg/mL concentration.

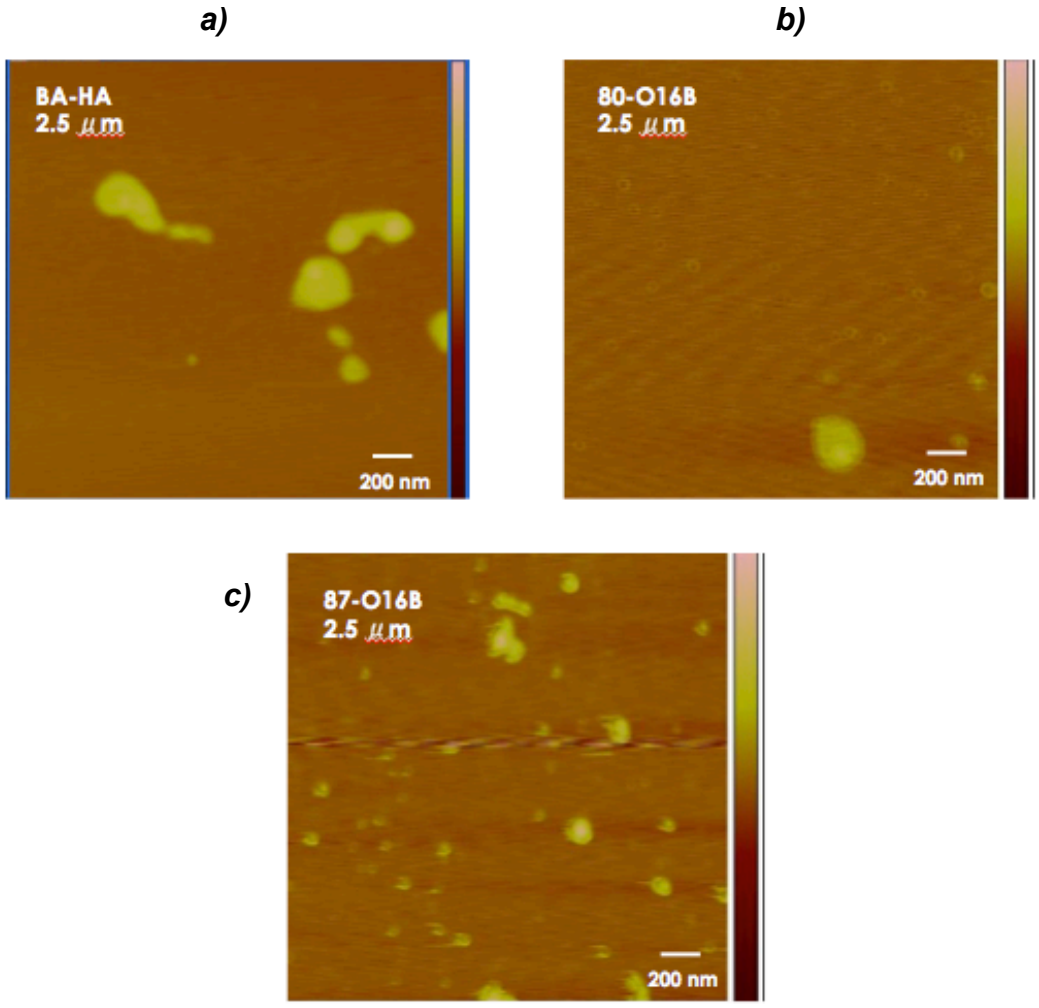

Figure 10 Height image of the a) BA-HA, b) 80-O16B, and c) 87-O16B captured by AFM imaging.

At 1 mg/mL, the AFM images show that the lipidoids have formed spherical micelles. This indicates that the CMC values for each lipidoid should be below 1 mg/mL. It can also be concluded that 87-O16B has the smallest particle sizes, less than approximately 100 nm, where as BA-HA and 80-O16B nanoparticles are more similar in size of approximately 200 nm.

4.3.2 CMC

4.3.2.1 Experimental Validation with Sodium Dodecyl Sulphate (SDS) CMC Measurement

The 1:3 ratio method by pyrene has been supported by many studies as an accurate as sensitive measurement of CMC. However, to ensure accuracy of the procedure within the lab and for this study, the CMC value for sodium dodecyl sulphate (SDS) was first measured. Dong et al. performed CMC measurements by similar fluorescence spectroscopy with pyrene observed two characteristics about the emission and excitation spectra: (i) There are four distinct peaks within 360 to 400 nm emission wavelength, and (ii) the proportional relationship between the surfactant concentration in the solution and the intensity of the spectrum peak [28]. In other words, as the surfactant concentration increased in the solutions, so did the intensity of the spectra peaks. **Figure 11** shows the emission and

excitation spectra of SDS that were observed at different concentrations ranging 5 mM to 11.5 mM. These results support the findings established by Dong et al. and thus, it can be concluded that the experimental protocol for determining CMC is sound and accurate.

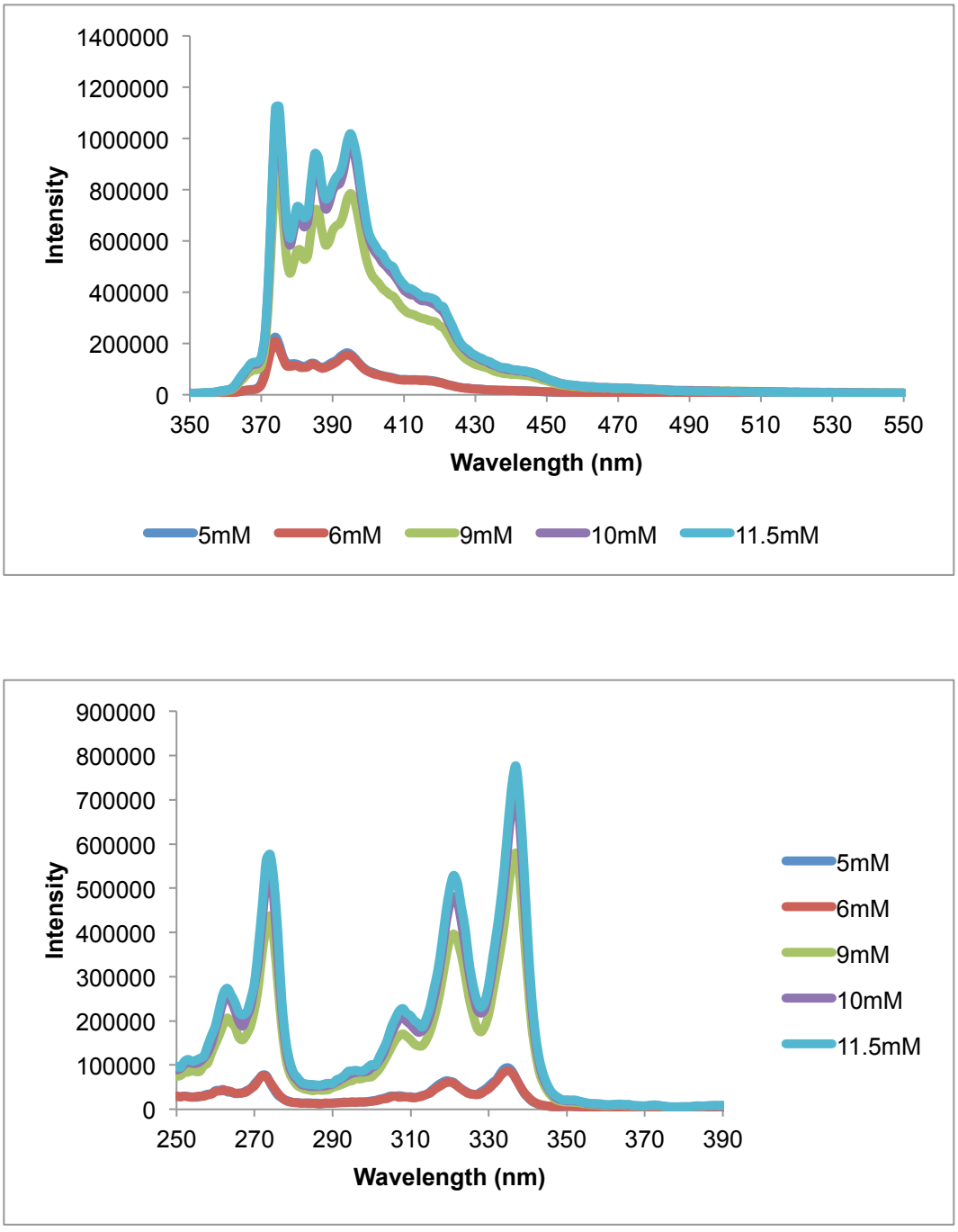

Figure 11 SDS spectra measured: a) Emission spectra, b) Excitation spectra

4.3.2.2 CMC of SDS

As previously discussed, many studies have shown that the 1:3 ratio as a function of surfactant concentration can be accurately modelled using the Sigmoidal Equation. Using OriginLab, the data obtained was successfully fitted against the sigmoidal model (**Figure 12**).

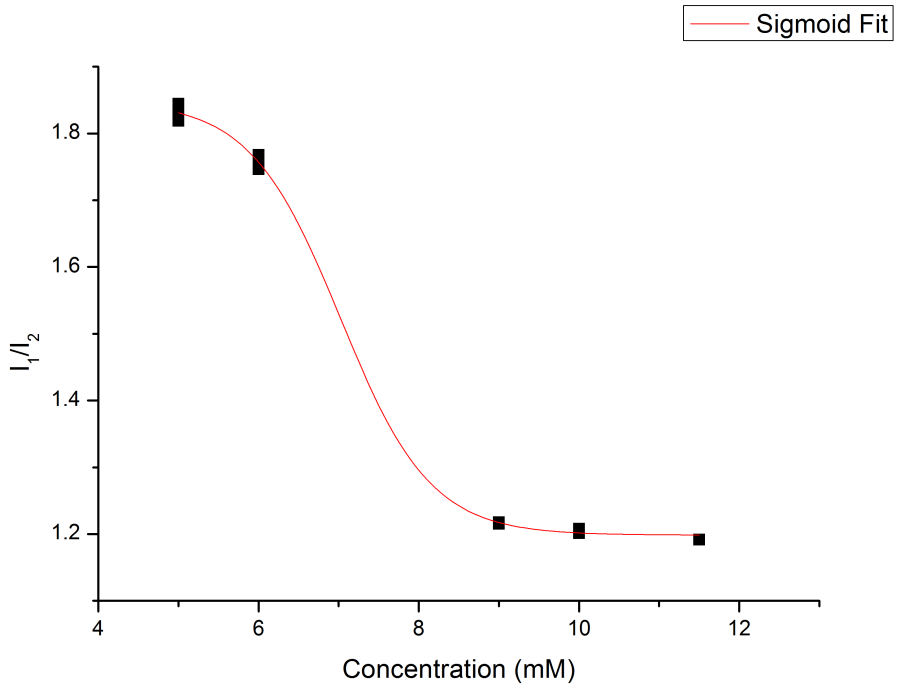

Figure 12 1:3 ratio plotted against SDS concentration and fitted against the Sigmoidal model.

The fitted results determined the CMC to be approximately 7.02 mM. This value is very close to the literature CMC values of SDS at 8.03 mM [33]. As a result, it is reasonable to assume the 1:3 ratio method used is feasible for future experiments.

4.3.2.3 CMC of the Zwitterionic Lipidoid and that of Existing Lipidoids

4.3.2.3.1 Effect of Lipidoid Concentration on the Emission Spectra and the 1:3 Ratio

Similar to SDS, the 1:3 ratio was determined from the emission and excitation spectra at each surfactant concentration and fitted against the Sigmoid model. In both the study conducted by Dong et al. and the measurement of SDS, an increasing intensity in the peak of the emission spectra was observed as its concentration in the solution increased [28]. Moreover, at concentrations above the CMC, the intensity of the emission spectra should be much larger than that for concentrations below the CMC. In contrast, the data gathered from this study shows the opposite trend (**Figure 13** and **Figure 14**).

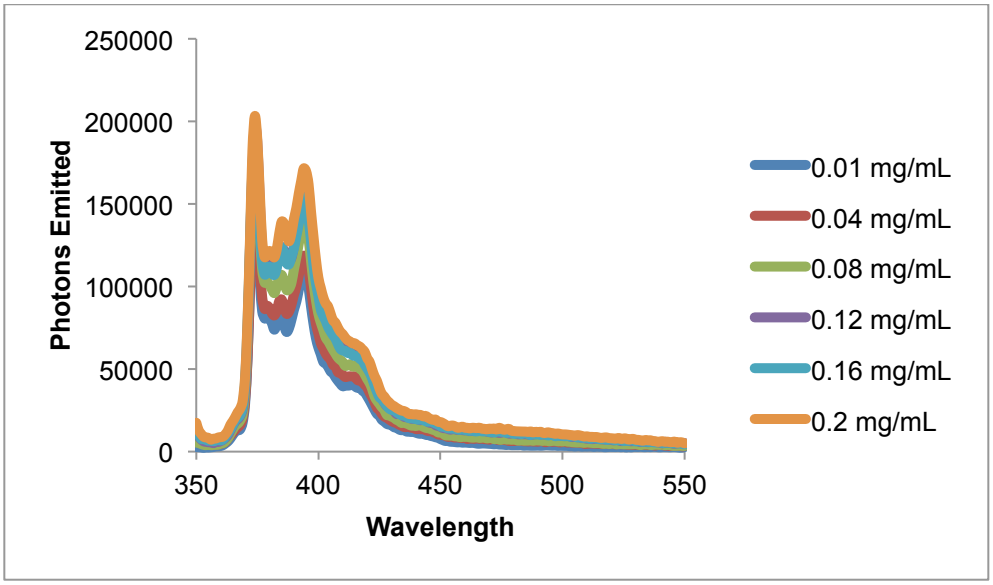

Figure 13 Emission spectra for BA-HA at various concentrations ranging from 0.01 mg/mL to 0.2 mg/mL.

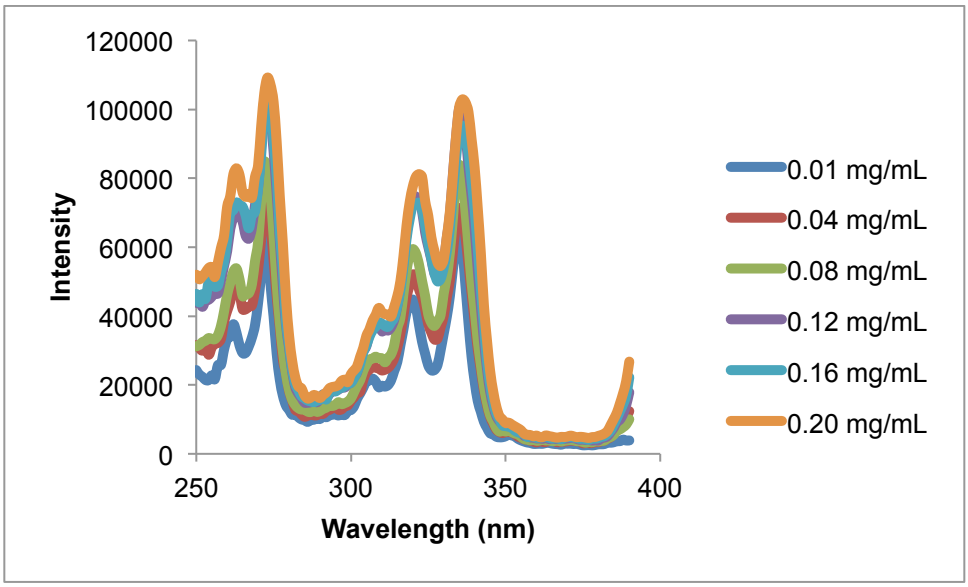

Figure 14 Excitation spectra for BA-HA at various concentrations ranging from 0.01 mg/mL to 0.20 mg/mL.

Many studies, such as one that was conducted by Cavalieri et al., also observed this phenomenon during their research on pyrene fluorescent quenching. The authors noted similar findings where the intensity of the emission spectra decreased as the surfactant concentrations increased. They attributed this pattern as a result of the two factors: the collisional quenching that occurs due to the surfactant molecules and the polarity of the microenvironment within the nanoparticles. The decrease in fluorescence intensity observed is indicative of the lipidoids weak tendency to self-assemble into the hydrophobic core [38]. In other words, the less polar the region within the micelles is, and thus smaller 1:3 ratio, the stronger the propensity for self-assembly of the lipidoids. Similar to the spectra, the 1:3 ratio decreased as the lipidoid concentration increased (**Figure 15**). This pattern was observed across all lipidoids that were

tested. The 1:3 ratio at different lipidoid concentrations closely resembles that of the Sigmoidal modal and can thus, be fitted against it and used to calculate the CMC of the corresponding lipidoid

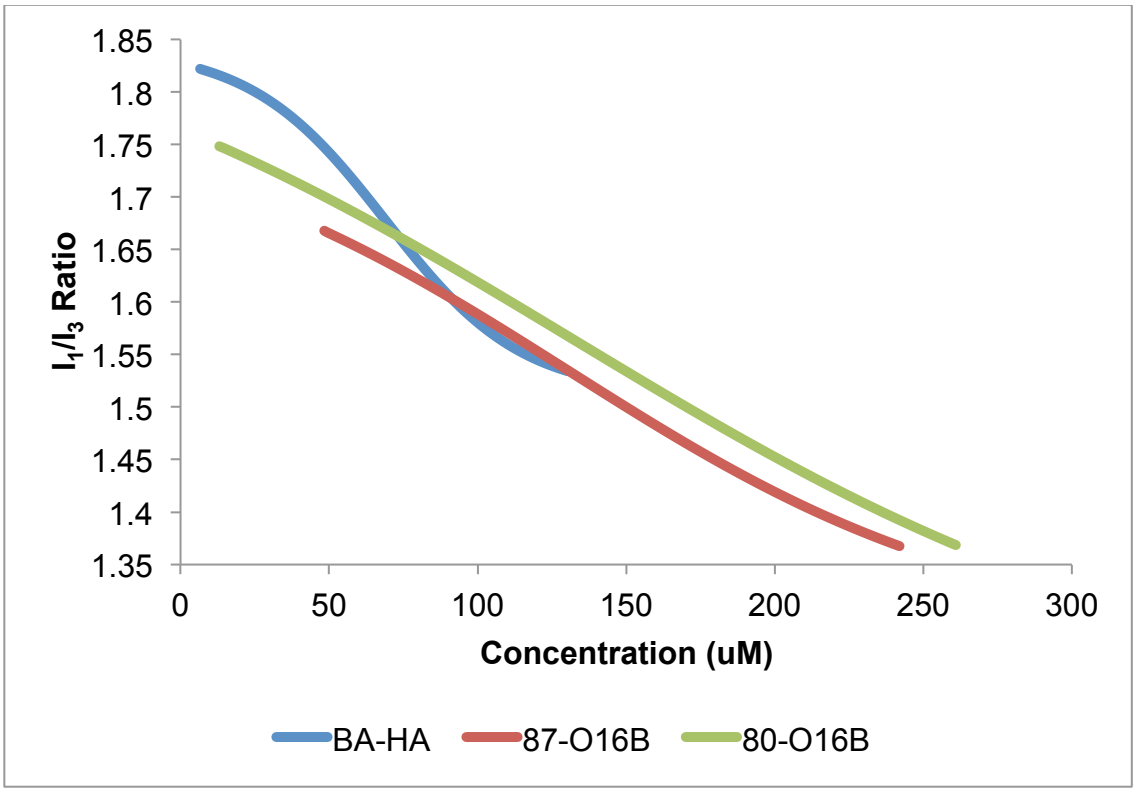

Figure 15 1:3 ratio of all lipidoids fitted against the Sigmodal model.

As previously stated, the 1:3 ratio is indicative of the polarity of the microenvironment within the nanoparticles. Thus, it is likely that the 1:3 ratio of the pyrene in different lipidoids may also be different. From the data, it is clear that the presence of the disulphide bond, such as in 87-O16B and 80-O16B, has an overall smaller 1:3 ratio. Another important note is that BA-HA has a much more drastic decrease in 1:3 ratio as the lipidoid concentration exceeds the CMC value, whereas 87-O16B and 80-

O16B exhibit a more gradual decrease in 1:3 ratio. This is likely due to the much larger chain length and molecular weight of the BA-HA lipidoid.

4.3.2.3.2 Lipidoid Structure and the Effect on its CMC

Similar with SDS, the 1:3 ratio was determined from the emission and excitation spectra at each surfactant concentration and fitted against the Sigmoid model. From the AFM results, it is expected that the CMC values of all the lipidoids should be less than 1 mg/mL, which was supported by the CMC tests. **Table 2** summarizes the CMC values for all lipidoids, as well as their structural properties such as length of carbon chain and the addition of a disulphide bond.

Table 2 CMC values measured for each lipidoid.

	Length of Alkyl Chain	Disulphide Bond	CMC Value (μM)
BA-HA	19	No	69
87-O16B	16	Yes	130
80-O16B	16	Yes	132

From **Table 2** two observations stand out. The first is that the “87” head group has a slightly lower CMC than that of the “80” head group. Secondly, the BA-HA lipidoid has a significantly lower CMC value, by at least half the value. The longer BA-HA alkyl chain lowers the CMC value due to the hydrophobic effect in which the hydrogen-bonding network becomes even stronger upon entering into the water molecules [32]. Moreover, the increase in the length of the chain causes the size of the micelles to

increase. As a result, few molecules are required in order to form the micelles. Previous research has shown that the presence of the disulfide bond also lowers the CMC value [35]. However the results show that despite the presence of disulfide bonds in both 87-O16B and 80-O16B lipidoids, their CMC values are still much larger than that of BA-HA. In this case, the effect of the longer alkyl chain of the BA-HA lipidoid outweighs the effects of having a disulfide bond.

The low CMC value of BA-HA makes it a very promising delivery vehicle as it means that the micelle is much more stable and requires a lower lipidoid concentration is needed to form the micelles [36].

To summarize, this study has shown that 1:3 pyrene is a sound method in determining the CMC value of lipidoids, the self-assembly of the lipidoids is greatly affected by the head group and the alkyl chain length of the lipidoid. As well, the propensity for self-assembly can be indicative of the polarity of the microenvironment in the micelles. In other words, the less polar the region within the micelles is, and thus smaller 1:3 ratio, the stronger the propensity for self-assembly of the lipidoids. From these results, it can be concluded that the structure of the lipidoids certainly has a large affect on its CMC value.

4.3.3 Particle Size

Having a solid understanding of the morphology and structure of the delivery vehicle is important to be able to optimize the release of the therapeutic load and prolong release in the body. DLS is known to possess high accuracy and the ability to measure extremely small particles. Thus, it was used to measure the particle sizes at a higher resolution than may be possible with AFM. For easier comparison, the data for the lipidoid particle sizes will be discussed in conjunction with the particle size data of the lipidoids encapsulated with DOX in Section 6.3.1.

Chapter 5: Biocompatibility Study

5.1 Introduction

There are many considerations that must be taken when developing drug delivery systems and many obstacles that must be overcome. Nanocarriers at the forefront of the industry are able to increase the solubility of poorly soluble drugs, be therapeutically efficient, minimize cytotoxicity, and increase pharmacokinetics profile and duration at the active site. These issues are difficult to overcome as there are still many aspects of the physiological environment of the cells, tissue and body that are not fully understood. It must also be clinically safe and not induce any undesirable biological or cellular responses. Thus, one way to test the robustness of a carrier is to examine its cytoxicity using a MTT assay. Well-defined nanocarriers will not induce any cellular or biological responses and have low cytotoxicity.

MTT uses fluorescence spectroscopy to measure cellular metabolic activity, and thus cell viability. It can be used as an indicator of how toxic the dosed substance is to the cells. The concept is based on the reduction of MTT by mitochondrial dehydrogenases, which causes both a colour change from yellow to purple and the formation of formazan crystals. The formazan product is then solubilized by dimethyl sulfoxide (DMSO) and the spectra of the cells can be measured at 570 nm using a spectrophotometer.

5.2 Materials and Method

5.2.1 Cell Culture and Lipidoid Preparation

The human prostate cancer cell line, PC-3 cell, was purchased from ATCC and cultured in RPMI1640 (Sigma Aldrich, St. Louis, MO) supplemented with 10% fetal bovine serum (Sigma Aldrich) and 1% penicillin. The cells were incubated under 5% CO_2 at 37°C. All lipidoids were synthesized and stored at 4°C until use. The lipidoid stock was prepared at 1 mg/mL in PBS for each lipidoid, as well as an additional stock solution of 3 mg/mL for BA-HA. Immediately prior to delivering the lipidoids, they were sonicated and vortexed until the solution was homogenous.

5.2.2 Pure Lipidoid Delivery and Cell Viability Assay

The cells were seeded in a 96 well plate at 5 K per well for 24 h before dosing. For 80-O16B and 87-O16B, the cells were dosed at concentrations ranging between 1-180 μg/mL and between 1-400 μg/mL for BA-HA. After 48h incubation, the cell media was removed and replaced with media containing 0.5 mg/mL thiazolyl blue tetrazolium bromide (MTT), purchased from Sigma Aldrich (St. Louis, MO). Cell media was then removed after 2 h incubation and the MTT was solubilized using dimethyl sulfoxide (DMSO). The cells were placed on a shaker for 10 minutes at a setting of 215 to ensure the DMSO is well mixed within the

wells. The absorbance was measured at 570 nm using a spectrophotometer.

5.2.2 Results and Discussion

As discussed, the MTT assay utilizes the reduction of MTT to cause a colour change that can be measured using a spectrophotometer and correlated to cell viability. The results indicate that the zwitterionic lipidoid, BA-HA, is significantly less toxic to the cells than the currently existing lipidoid library (**Figure 16**). Moreover, the decline in cell viability as the lipidoid dosage increases is much more gradual than in the 87-O16B and 80-O16B.

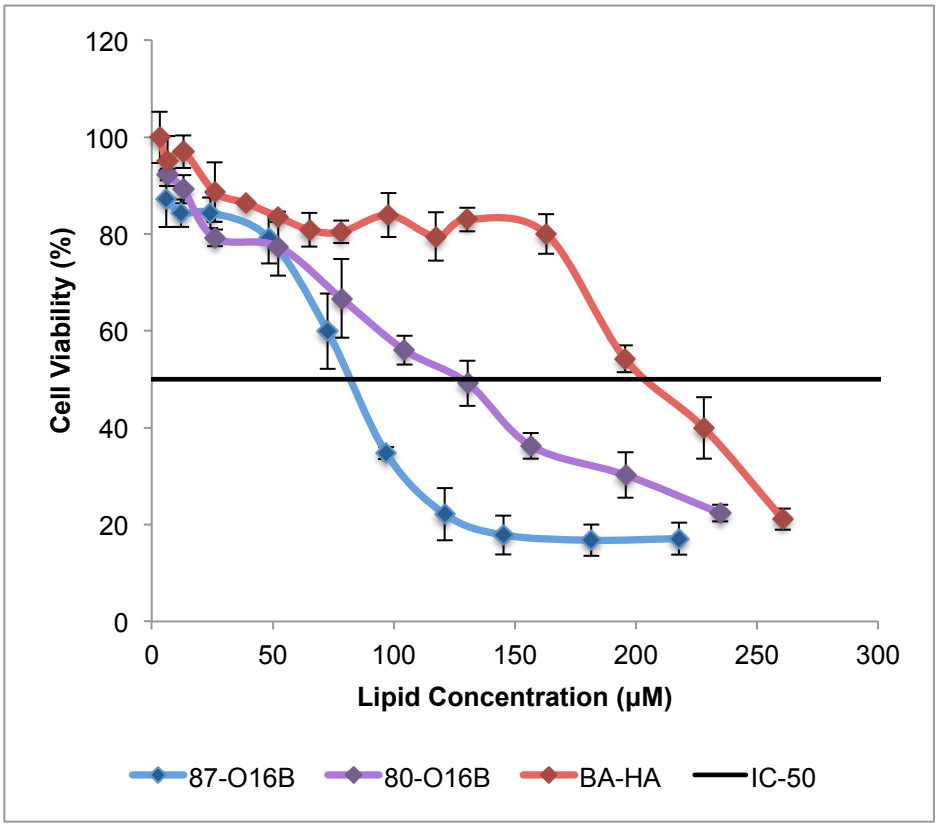

Figure 16 Cell viability of the lipidoids after 24 h incubation. BA-HA shows significantly less toxicity than the currently lipidoid library.

The MTT assay was performed in triplicates and then averaged to obtain precise data. For each test, the IC-50 was graphically determined and then averaged. BA-HA has an IC-50 value of approximately twice that in comparison to 87-O16B and 80-O16B (**Table 3**). In other words when dosed with concentrations higher than 206.8 ± 8.14 μM of BA-HA, only 50% of the cells remain viable after 48 h of incubation. The zwitterionic lipidoid is only toxic to the cells at extremely high concentrations.

Lipids	MW (g/mol)	Average IC-50 (μg/mL)	STDEV (μg/mL)	Average IC-50 (μM)	STDError (μM)
87-O16B	1156	72.5	6.61	87.7	8.00
80-O16B	1446	93.8	7.62	122.4	9.94
BA	827	317.5	12.50	206.8	8.14

Table 3 Averaged IC-50 values for all lipidoids. Performed in triplicates.

Although the concept of amino acid based zwitterionic lipidoids has been studied, BA-HA lipidoid exhibits extremely low cytotoxicity even in comparison to other zwitterionic lipidoids currently cited in literature. For instance, Obata et al. conducted a similar study synthesizing pH-sensitive amino-acid based zwitterionic lipids and their lipids achieved a cell viability of 60% at 100 ug/mL, which is 20% lower than what was observed in this study [38]. These results make BA-HA a very promising candidate for biomedical applications and further emphasizes the need to continue to expand the synthesis of a zwitterionic lipidoid library.

Chapter 6: Drug Encapsulation (DOX as a Model)

6.1 Introduction

To test the efficacy of the zwitterionic lipidoid as a drug carrier, the anti cancer drug doxorubicin was used as a model and encapsulated within the nanoparticles. Doxorubicin (DOX) is the most widely known and used anthracycline antibiotic group of anticancer drugs, commonly used in the treatment of haematological and solid tumours. Its therapeutics effects are largely limited by its risk of cardiomyopathy that can eventually result in congestive heart failure and death, which affects 2% of patients who receive lifetime doxorubicin doses of 450-500 mg/m^2 [37]. Doxorubicin's hydrophobic nature and its issues with causing acute and chronic toxicity make it a good candidate for lipdoid encapsulation as a model in this study.

6.2 Materials and Methods

6.2.1 Preparation of the Free-Base Doxorubicin (DOX)

The salt form of doxorubicin (DOX•HCl) was obtained from Sigma Aldrich (St. Louis, MO) and needed to be desalted into its free-base form before using for further tests. As many studies have done, DOX•HCl was mixed with triethylamine (TEA) (Sigma Aldrich, St. Louis, MO) in excess at a 1:2 molar ratio with DMSO and stirred over night [39][40] and then stored at 4°C. The final concentration of the stock solution of free-base dox was at 20 mg/mL.

Before encapsulating the drug into the lipidoids, it is important to first understand the characteristics of the drug itself, such as its emission spectrum and where the characteristic peaks lie. Moreover, a standard curve for which the unknown concentrations can be compared against needs to be generated.

6.2.2 Standard Curve

The doxorubicin standard curve was generated by diluting the stock solution of free-base DOX in DMSO at various known concentrations and then measuring their corresponding absorbance between 400-600 nm. The characteristic peak of doxorubicin was observed at 485 nm and so, the standard curve was made using the absorbance at that wavelength. With the measured absorbance obtained in future tests, the standard curve will be used to determine unknown concentrations of doxorubicin encapsulated within the lipidoids.

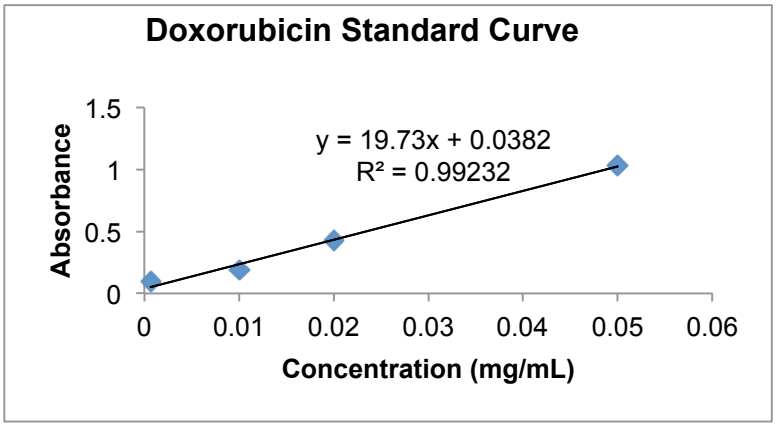

Figure 17 Free-base doxorubicin standard curve in DMSO.

6.2.3 Doxorubicin Encapsulation into Lidpidoid

To encapsulate the DOX into the lipidoids, the stock solution of free-base DOX was mixed with pure lipid such that a lipidoid to drug ratio of 10:2 wt/wt was maintained. According to Abraham et al., this is a common lipid to drug ratio for doxorubicin encapsulations [37]. The DOX-lipidoid solution was then added drop-wise into DI water to obtain a final lipidoid and drug concentration of 1 and 0.2 mg/mL, respectively. The solution was stirred with a magnetic bar for 10 minutes and dialyzed for 2 h to remove the DMSO and any DOX free drug. The water was removed and replaced after 1 h. The final DOX encapsulated lipidoid was either stored at 4°C or used immediately.

6.2.4 Drug Loading Content (DLC) and Drug Loading Efficiency (DLE) of Doxorubicin-Encapsulated Zwitterionic Lipidoid

After synthesizing and preparing the DOX-encapsulated lipidoids, the drug loading content (DLC) and drug loading efficiency (DLE) calculated using absorbance measurements taken using a spectrophotometer at 485 nm. The samples were prepared immediately prior to taking measurements by diluting the DOX-encapsulated lipidoids in DMSO at 1:10 ratio and transferred to a quartz cuvette. The standard curve can then be used to

determine the concentration of drug encapsulated using the absorbance values measured. Knowing the initial concentration and volume of the drug loaded, and thus their mass, the following formula can be used in conjunction with the measured data to calculate the DLC and DLE:

$$\mathrm{DLC} = \frac{\text{Measured Drug Concentration} \times \text{Measured Drug Volume}}{\text{Measured Drug Concentration}} \times 100\% \quad (2)$$

$$\mathrm{DLE} = \frac{\text{Measured Drug Concentration} \times \text{Measured Drug Volume}}{\text{Original Mass of Drug}} \times 100\% \quad (3)$$

6.2.5 Cytotoxicity of Encapsulated Lipidoid Nanoparticles

The materials and procedure to measure the cytoxicity of the DOX encapsulated lipidoid nanoparticles is the same as that previously used in **Section 5.2.1** and **Section 5.2.2**, however the concentration of DOX encapsulated lipidoid delivered to the cells ranged between 0.25-400 μg/mL.

6.3 Results and Discussion

6.3.1 Physical Characterization

6.3.1.1 Particle Size

The morphology of the lipid nanoparticles was observed by AFM and the particle sizes could be estimated from the images. However, DLS provides a more accurate representation of the particle sizes using light scattering

and can measure as small as 1 nm. The pure lipidoids, as well as those encapsulated with DOX, were diluted at a 1:100 ratio in DI water and DLS measurements were taken. The results show that BA-HA is slightly smaller in size in comparison to the other lipidoids and maintains a similar size after encapsulating with DOX (**Figure 18**). An interesting observation to note is the slight decrease in size of the 87-O16B and 80-O16B nanoparticles once encapsulated with DOX. This likely due to the strong binding forces between the hydrophobic DOX and the cationic lipid

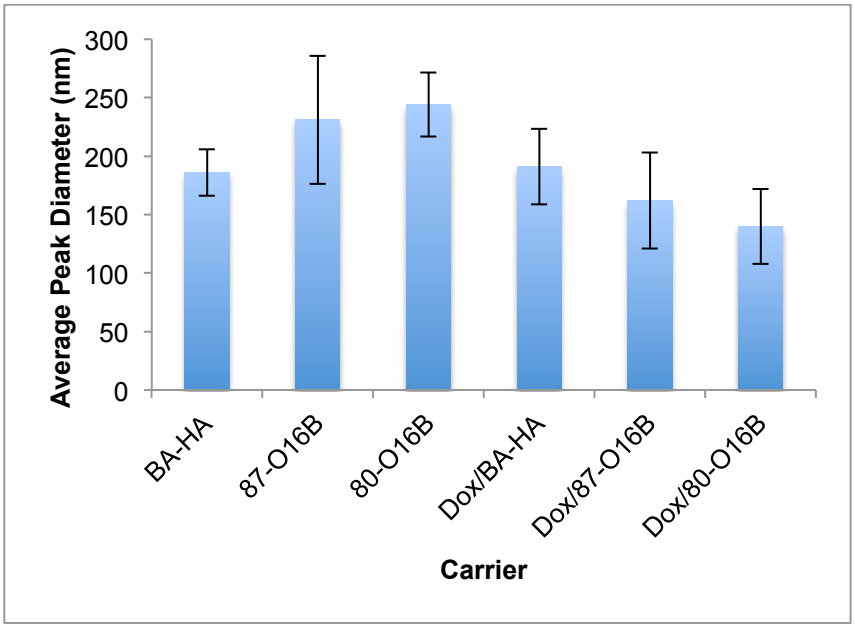

Figure 18 Average peak diameter of BA-HA, 87-O16B, 80-O16B lipidoid nanoparticles and their nanoparticles when encapsulated with DOX.

Table 4 summarizes the average peak diameters and the polydisperisty measured for each lipidoid and their DOX-encapsulated counterpart. In contrast to the particle size estimates from the AFM images, DLS

measurements shows that the BA-HA lipidoid is approximately a third of the diameter of the 87-O16B and 80-OB16B lipidoids. This may be due to several reasons. Perhaps the particles captured from that particular AFM image captured was slightly larger and was not an accurate reflection on majority of the BA-HA nanoparticles. In a review about DLS measurements in small particles in liquids, Pecora explained that particles in liquid dispersion are very sensitive and their properties can be altered when drying or placed on a surface [29]. This could be another reason for the discrepancies in measured particle sizes as samples of the lipid nanoparticles had to be transferred onto silica wafers and dried.

Table 4 Average peak diameter and the polydisperisty of BA-HA, 87-O16B, and 80-O16B lipidoid, as well as the sizes and polydisperisty once encapsulated with DOX.

Lipid	Average Peak Diameter (nm)	Standard Deviation of Average Peak Diameter (nm)	Mean Polydispersity	Standard Deviation of Mean Polydispersity
BA-HA	186	19.8	0.274	0.0357
87-O16B	231	54.7	0.219	0.062
80-O16B	244	27.4	0.074	0.04
DOX/BA-HA	191	32.4	0.254	0.0567
DOX/87-O16B	162	41.0	0.13	0.0603
DOX/80-O16B	140	32.2	0.284	0.0363

6.3.2 Doxorubicin Encapsulation into Lidpidoid

The final DOX-encapsulated lipid nanoparticles had a drug and lipid concentration of 0.2 and 1 mg/mL, respectively. A red aqueous solution made up the DOX-encapsulated lipid nanoparticles, with the DOX/BA-HA nanoparticles having a slightly brighter and clearer appearance. This contrasted the slightly cloudier and dull appearance of the DOX/87-O16B and DOX/80-O16B samples **(Figure 19).**

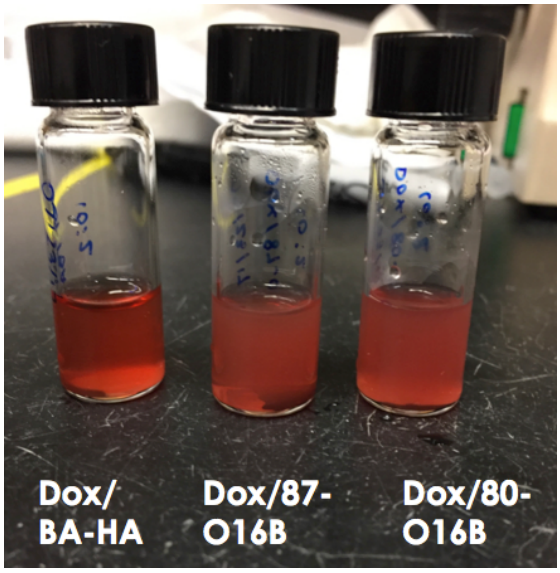

Figure 19 DOX/Lipidoid samples at a final drug and lipidoid concentration of 0.2 and 1 mg/mL, respectively.

The concentration of drug encapsulated within the lipid nanoparticles was determined using a spectrophotometer at the doxorubicin characteristic wavelength of 485 nm. Using the DOX standard curve, the measured absorbance values could be related to the concentration of drug encapsulated. The concentration of encapsulated DOX in the lipid nanoparticles are comparable across all lipidoids **(Figure 20).** The

negative control (NC) consisting of lipid only measurements show that the lipidoids had no interference with measurements.

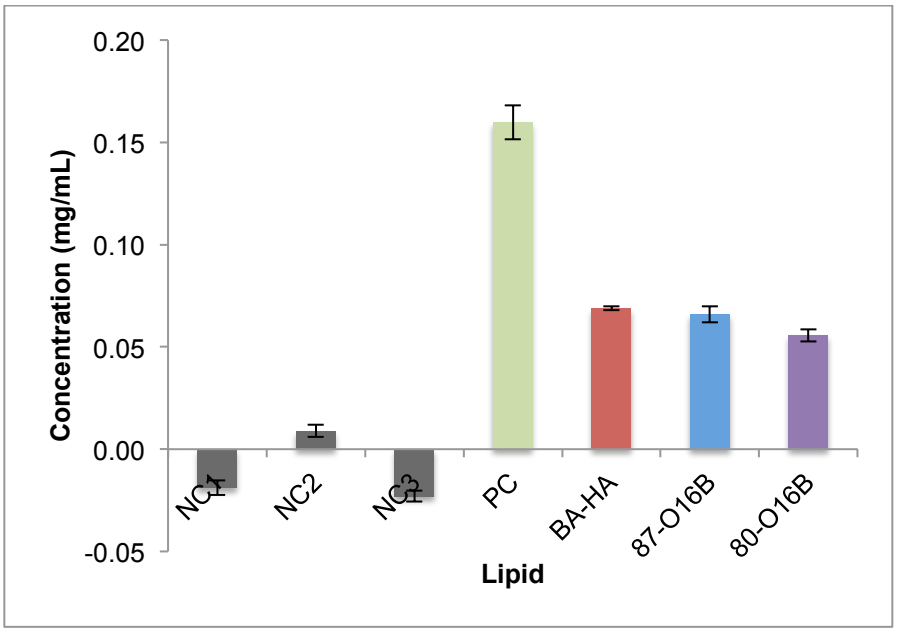

Figure 20 Concentration of DOX encapsulated in BA-HA, 87-O16B, and 80-O16B lipidoids. Positive control (PC): Free DOX, Negative control (NC): NC1: BA-HA only, NC2: 87-O16B only, NC3: 80-O16B only. Performed in triplicates.

Using the measured data, the DLC and DLE of the DOX-encapsulated lipidoids was then calculated **Equation 2** and **Equation 3**. The amount of DOX encapsulated into the lipid nanoparticles is fairly low with none of the lipids able to encapsulated concentrations even half that of the positive control (PC) free-base DOX (**Table 5**).

Table 5 The concentration of DOX encapsulated in the lipid nanoparticles and their corresponding DLC and DLE values. NC (Negative control). NC1: BA-HA only, NC2: 87-O16B only, NC3: 80-O16B.

Lipid	NC1	NC2	NC3	PC	BA-HA	87-O16B	80-O16B
Average Concentration (mg/mL)	-0.01875	0.00894	-0.0230	0.1598	0.0690	0.0660	0.0557
DLC (%, mg/mg)					9.68	9.29	7.91
DLE (%, mg/mg)					34.5	33.0	27.9
STDError Concentration (mg/mL)	0.00362	0.00302	0.00262	0.00839	0.00099	0.00366	0.00251
STDError DLC (%, w/w)					0.128	0.483	0.339
STDError DLE (%, w/w)					0.494	1.83	1.25

Again, the DLC across all lipidoids are quite comparable with the DLC of BA-HA being only slightly higher than that of 87-O16B, followed by 80-O16B with the smallest amount of DOX. In terms of DLE, the results were even more similar and within the standard error, it's difficult to say there is any discernable between the efficiencies of each lipidoid. Previous research, such as those conducted by Nguyen-Van et al., Yuan et al., and H show that the DLC values for BA-HA and 87-O are able possess higher than or comparable encapsulate DOX [41][42][43].

Optimization of the formulation is necessary to achieve greater results. One factor affecting the encapsulation ability is the aqueous entrapment [44]. According to Bhai et al. more drug is can be encapsulated with a larger aqueous volume. They reason that due to the larger volume of

aqueous space within the multiple compartment liposomes, there can be a much higher percentage of drugs encapsulated than in the single compartment vesicles. This is also supported by the notion that non polar drugs, such as DOX, aggregate to the internal aqueous parts of the liposomes, in addition to binding to the liposome membrane [45]. Future tests can consider incorporating charged lipids such as phosphatidyl serine into the bilayers, or utilizing osmotic swelling to increase the aqueous volume in the liposomes.

Another factor that can affect the degree of drug entrapment is the lipid-drug ratio of the formulated lipid nanoparticles. According to Ramana et al. a decrease in the lipid-drug ratio decreases the size of the lipid nanoparticles. As a result, the aqueous volume is reduced causing the encapsulation efficiency to also decrease [46]. The authors also noted that an increase in the lipid-drug ratio, increased the amount of drug loaded. In the formulations with the zwitterionic lipidoids and current lipidoid library, a lipid-drug ratio of 10:2 wt/wt was used. Future tests should increase the lipid-drug ratio, such as to 5:1, and observe any changes in the DLC and DLE. Ramana et al. also noted that up to a lipid-drug ratio of 5:1, the amount of drug loaded no longer increased beyond this ratio. Thus, if the lipid-drug ratio was increased to 5:1, it would be expected that only the encapsulation efficiency would improve.

6.3.3 Cytotoxicity

Similar to the cell viability test conducted on the lipidoids, the cell viability of the DOX-encapsulated lipid nanoparticles was also examined. The BA-HA lipdoids possessed the highest IC-50 amongst the lipidoids tested previously. Therefore, it is expected that the BA-HA lipid nanoparticles encapsulated with the DOX will also exhibit the lowest cyotoxicity. From **Figure 21** , it is clear that this is the case and BA-HA has significantly lower cells inhibited by the BA.

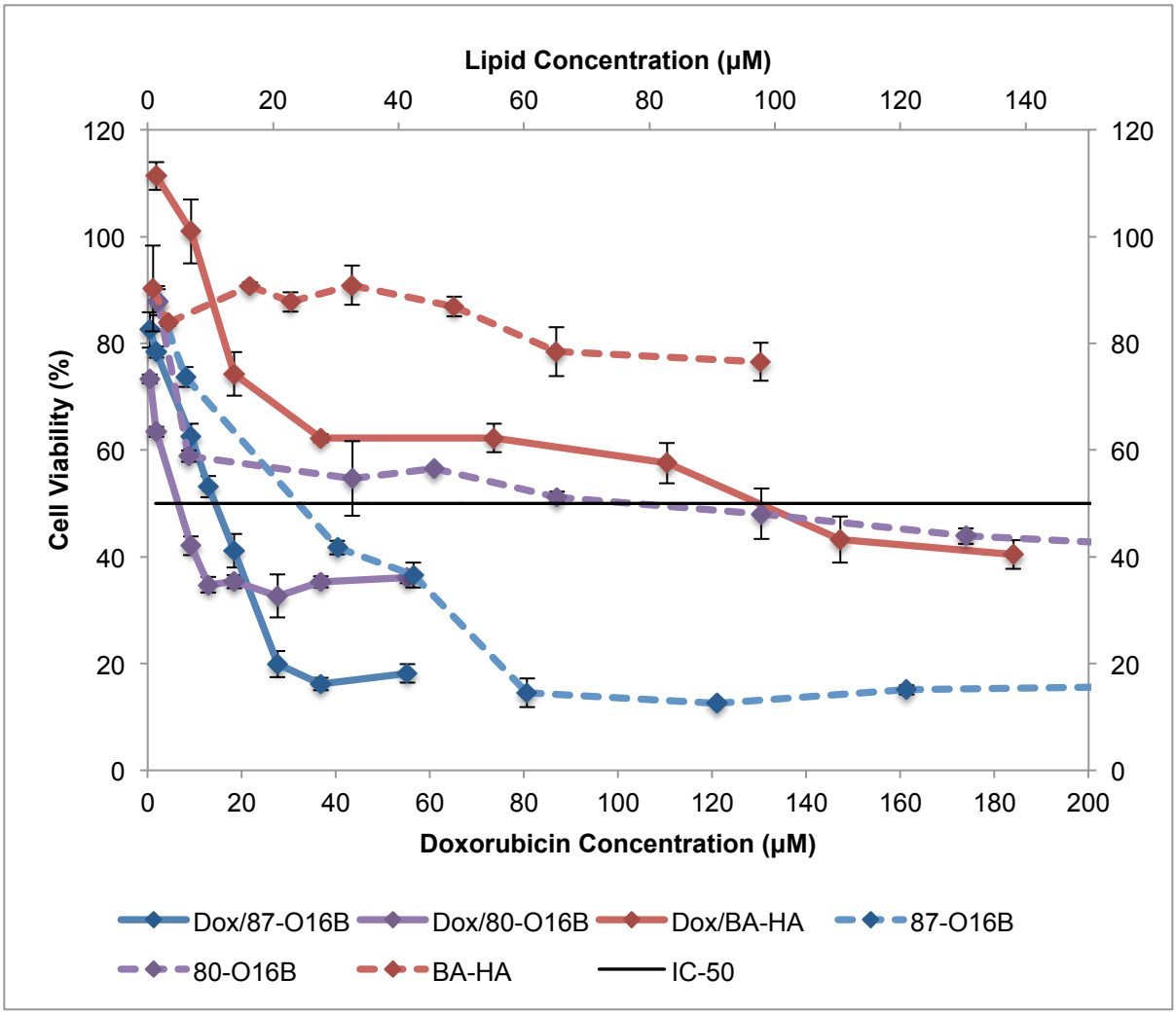

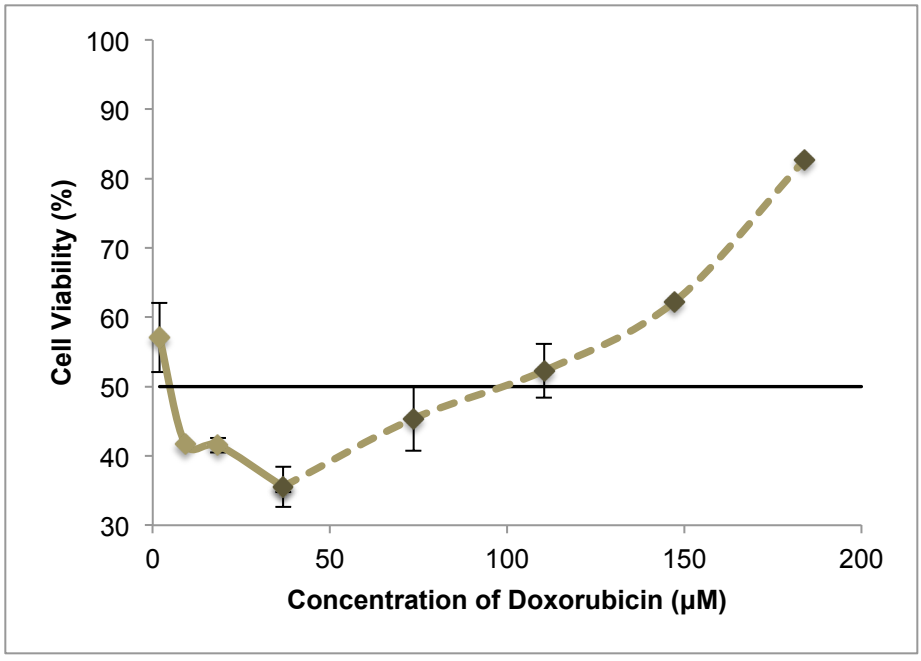

Figure 21 Top (a): Cell viability of DOX-encapsulated lipid nanoparticles in BA-HA, 87-O16B, and BA-HA. Dashed lines represent the negative control of lipid only deliveries. **Bottom (b):** Cell viability for positive control deliveries of free DOX. Dashed lines represent inaccurate measurements recorded where the red colour of DOX begins to interfere with accurate absorbance, and thus cell viability readings.

As more DOX-lipid nanoparticles are delivered to the PC-3 cells, the cell viability will naturally continue to decrease in cell viability as there are greater foreign bodies being introduced to the cells. However, in the positive control tests with free DOX, the absorbance values, and thus the cell viability measurements, suddenly increased drastically beyond approximately 74 μM of DOX being dosed as shown in the **Figure 20B** indicated by the dashed lines.

It is believed that these results were due to the red colour of the DOX drug interferring with the absorbance readings. Any measurements taken after that point is unreliable. Despite removing and replacing the media prior to adding MTT, free DOX remains in the either on the sides of the wells or attached the to cells. In order to resolve this issue, the cells should be washed with PBS twice prior to adding the MTT to remove any free DOX that may interfer with the reading. It is believed that these results were due to the red colour of the DOX drug interferring with the absorbance readings. Any measurements taken after that point is unreliable. In fact, experiments were conducted with the new procedure including the PBS washes, however because the cells had been passaged too many times they were became increasingly unhealthy and provided unreliable results. Due to time constraints, the positive control tests could not be repeated with the PBS washes for the higher concentrations.

All MTT assays were performed in triplicates and then averaged to obtain precise data. For each test, the IC-50 was graphically determined and then averaged. DOX/BA-HA lipid nanoparticles have an IC-50 value of almost a hundred times greater than that of the 87-O16B and 80-O16B encapsulated nanoparticles. This is especially evident in the tabulated summary of the IC-50 values in **Table 6**.

Table 6 Averaged IC-50 values for DOX-encapsulated lipid nanoparticles.

	Average IC-50 (μM)
Free DOX	8.74
DOX/87-O16B	14.3
DOX/80-O16B	5.98
DOX/BA-HA	128.5

As expected, the DOX encapsulated in the BA-HA lipidoid produced the lowest toxicity among the lipidoids. The results show free DOX is quite toxic alone and we see that it becomes slightly less toxic when encapsulated in 87-O16B. However, when encapsulated in BA-HA it becomes significantly less toxic.

The zwitterionic lipidoid, BA-HA, is able to successfully encapsulate the doxorubicin and reduce its cytotoxic effects at a significantly in comparison to previous studies. Obata et al. encapsulated their amino acid based zwitterionic lipidoid with doxorubicin at a drug to lipid 10:1 wt/wt ratio.

After 24 h of incubation, they observed IC-50 of approximately 3.5 and 4.5 ug/mL, or 8 and 12 μM respectively. Their results are similar to that which was measured in this study when encapsulating within the existing lipidoids 87-O16B and 80-O16B.

To summarize, we have shown that the zwitterionic lipidoid BA-HA that was synthesized is by itself has extremely low toxicity and can successfully encapsulate a hydrophobic toxic drug. As well once encapsulated with the drug, the lipid nanoparticles can reduce its cytotoxic effects by 100 times in comparison to similar existing lipidoids.

Chapter 7: Future Perspective and Future Work

7.1 Summary

To summarize, the goal of this thesis is to initiate the development of a new library of Zwitterionic lipidoids and anlyze their physical and chemical properties to assess their potential in biomedical applications. Although amino acid based zwitterionic lipidoids have been studied, the use of β-alanine as polar head group has not be done. Its resulting zwitterionic lipidoid produced significantly lower cytotoxicity in comparison to current literature and makes this a novel approach to drug delivery. Future research will continue to expand the Zwitterionic lipidoid library and screen their potential for drug and protein delivery by exaiming their bicompatibility and delivery abilties.

Through Michael's addition, Zwitterionic lipidoids were successfully synthesized (BA-HA and 5A-HA) with their structural identities confirmed by NMR. Initially, four amino acids were selected for the synthesis of this library, however T-HA and OPA-HA lipidoids were unable to be dissolved and purified for use. As well due to time constraints, this study only focused on one zwitterionic lipidoid.

Physical characterization of the lipidoids was performed including AFM, CMC measurements, and particle size. AFM imaging was conducted to observe the morphology of the lipidoids and was measured using 1 mg/mL

samples. The images showed multiple spherical micelles formed and supported the notion that the formation of micelles occur at lipidoid concentrations beyond the CMC value. Particle size measurements indicated that the lipidoids were very similar in size, with BA-HA only slightly smaller than the other lipidoids with an average peak diameter of 186 nm in the pure lipid formulation and slightly higher in comparison when encapsulated with DOX at 191 nm.

Using the 1:3 ratio pyrene method, the CMC for the zwitterionic lipidoid was measured and compared with the existing lipidoid library, 87-O16B and 80-O16B. Preliminary experiments was conducted with SDS to validate the procedure was feasible for measuring CMC values for surfactants. BA-HA was shown to have the lowest CMC value among the lipidoids test, with almost half the value of the others (69 μm). The low CMC value means that a smaller amount of lipidoid is needed to form the micelles. Moreover, the micelles are much more stable and can encapsulate a greater amount of cargo within the micelles. The lower CMC value exhibited by BA-HA is likely attributed to the larger number of alkyl chains which results in a bigger micelle size and means less molecules are needed to form the micelle [40].

The lipidoids were then encapsulated with DOX at a DOX and lipidoid concentration of 0.2 and 1 mg/mL, respectively, while maintaining a 10:2

drug to lipid ratio. The drug loading efficiency (DLE) among all the lipidoids was fairly low where each lipidoid encapsulated at around 30% efficiency. However, the results show that each lipidoid was able to successfully encapsulate DOX at comparable DLC values cited in literature.

Lastly, cell viability was then conducted on both pure lipidoids and those encapsulated with DOX. BA-HA showed extremely low cytoxocity with IC-50 (208.6 μM) levels twice as high than that of the current lipidoid library. The differences were even more dramatic when BA-HA was encapsulated with DOX, where BA-HA had IC-50 values that were ten times greater (128.5 μM).

Through this thesis study, it is clear that BA-HA has significant potential as a candidate for biomedical applications. The low toxicity of the zwitterionic lipidoid rivals that which is seen in literature and can used to reduce cytotoxic effects to normal tissues. As well, its low CMC value means the lipidoid is more stable and has the potential to encapsulate a greater load. The particle size is comparable to existing lipidoids which means it can be delivered into the small regions in the tissues and have longer therapeutic release.

7.2 Future Perspective and Direction

Future work should focus on expanding the zwitterionic lipidoid library. For instance, the library can explore the use of degradable lipidoids or those with varying degree of saturation. BA-HA has shown there is a lot of potential in this area of drug delivery and this study has shown that cause worth pursuing. Zwitterionic lipidoids are known to have low adhesion, longer circulation in the blood, and greater stability. Thus, a more in depth biocompatibility study can be conducted to include hemolysis, adhesion tests, and stability tests. Adhesion tests can be performed using solution depletion techniques, spectroscopy (fluorescence spectrscopy, infrared absorption, Raman scattering), or by using optical tehcniques (ellipsometry, surface plasmon resonance, etc). The encapsulation of BA-HA can also be optimized to improve its efficiency and loading. For instance, drug:lipid ratio has been shown by previous research to have a great effect the ability to encapsulate.

References

[1] Shao, Qing, and Shaoyi Jiang. 2015. “Molecular Understanding and Design of Zwitterionic Materials.” Advanced Materials 27 (1): 15–26. doi:10.1002/adma.201404059.

[2] Zheng, Liuchun, Zhijuan Sun, Chuncheng Li, Zhiyong Wei, Priyesh Jain, and Kan Wu. 2017. “Progress in Biodegradable Zwitterionic Materials.” Polymer Degradation and Stability 139 (May): 1–19. doi:10.1016/j.polymdegradstab.2017.03.015.

[3] Jin, Qiao, Yangjun Chen, Yin Wang, and Jian Ji. 2014. “Zwitterionic Drug Nanocarriers: A Biomimetic Strategy for Drug Delivery.” Colloids and Surfaces B: Biointerfaces 124 (December): 80–86. doi:10.1016/j.colsurfb.2014.07.013.

[4] Kondo, Takuya, Kouji Nomura, Makoto Gemmei-Ide, Hiromi Kitano, Hidenori Noguchi, Kohei Uosaki, and Yoshiyuki Saruwatari. 2014. “Structure of Water at Zwitterionic Copolymer Film–liquid Water Interfaces as Examined by the Sum Frequency Generation Method.” Colloids and Surfaces B: Biointerfaces 113 (January): 361–67. doi:10.1016/j.colsurfb.2013.08.051.

[5] He, Yi, Jason Hower, Shengfu Chen, Matthew T. Bernards, Yung Chang, and Shaoyi Jiang. 2008. “Molecular Simulation Studies of Protein Interactions with Zwitterionic Phosphorylcholine Self-Assembled Monolayers in the Presence of Water.” Langmuir 24 (18): 10358–64. doi:10.1021/la8013046.

[6]H. Farhood, N. Serbina, and L. Huang, “The role of dioleoylphosphatidylethanolamine in cationic liposome mediated gene transfer,” Biochimica et Biophysica Acta, vol. 1235, no. 2, pp. 289–295, 1995.

[7] H. Farhood, X. Gao, K. Son et al., “Cationic liposomes for direct gene transfer in therapy of cancer and other diseases,” Annals of the New York Academy of Sciences, vol. 716, pp. 23–35, 1994.

[8] S. Sim˜oes, V. Slepushkin, R. Caspar, M. C. Pedroso de Lima, and N. D¨uzg¨unes¸, “Gene delivery by negatively charged ternary complexes of DNA, cationic liposomes and transferrin or fusigenic peptides,” Gene Therapy, vol. 5, no. 7, pp. 955–964,1998

[9] Balazs, Daniel A., and Wt. Godbey. 2011. “Liposomes for Use in Gene Delivery.” Journal of Drug Delivery 2011: 1–12. doi:10.1155/2011/326497.

[10] I. Koltover, T. Salditt, J. O. R¨adler, and C. R. Safinya,“An inverted

hexagonal phase of cationic liposome-DNA complexes related to DNA release and delivery," Science, vol. 281, no. 5373, pp. 78–81, 1998

[11] I. S. Zuhorn, U. Bakowsky, E. Polushkin et al., "Nonbilayer phase of lipoplex-membrane mixture determines endosomal escape of genetic cargo and transfection efficiency," Molecular Therapy, vol. 11, no. 5, pp. 801–810, 2005.

[12] N. J. Zuidam and Y. Barenholz, "Electrostatic and structural properties of complexes involving plasmid DNA and cationic lipids commonly used for gene delivery," Biochimica et Biophysica Acta, vol. 1368, no. 1, pp. 115–128, 1998.

[13] Gao, Weiwei, Che-Ming J. Hu, Ronnie H. Fang, and Liangfang Zhang. 2013. "Liposome-like Nanostructures for Drug Delivery." Journal of Materials Chemistry B 1 (48): 6569. doi:10.1039/c3tb21238f.

[14] Altınoglu, Sarah, Ming Wang, and Qiaobing Xu. 2015. "Combinatorial Library Strategies for Synthesis of Cationic Lipid-like Nanoparticles and Their Potential Medical Applications." Nanomedicine 10 (4): 643–57. doi:10.2217/nnm.14.192.

[15] Nair DP, Podgórski M, Chatani S et al. The thiol-michaeladdition click reaction: a powerful and widely used tool inmaterials chemistry. Chem.

Mater. 26(1), 724–744 (2013).

[16] Sun, Shuo, et al. "Combinatorial library of lipidoids for in vitro DNA delivery." Bioconjugate chemistry23.1 (2011): 135-140.

[17] Wang, Ming, et al. "Enhanced Intracellular siRNA Delivery using Bioreducible Lipid‐Like Nanoparticles." Advanced healthcare materials 3.9 (2014): 1398-1403.

[18] Wang, Ming, et al. "A combinatorial library of unsaturated lipidoids for efficientintracellular gene delivery." ACS synthetic biology 1.9 (2012): 403-407.

[19] Sun, Shuo, et al. "Combinatorial library of lipidoids for in vitro DNA delivery." Bioconjugate chemistry23.1 (2011): 135-140.
Zhong, Q., et al. “Fracture polymer/silica fiber surface studied by tapping mode atomic forec microscopy.” Surface Science Letters. 290.1 (1993): L688-L692.

[20] Wang, Ming, et al. "Combinatorially Designed Lipid‐like Nanoparticles for Intracellular Delivery of Cytotoxic Protein for Cancer Therapy."Angewandte Chemie 126.11 (2014): 2937-2942.

[21] Wang, Ming, and Qiaobing Xu. "Combinatorial cationic lipid-like nanoparticles for efficient intracellular cytotoxic protein delivery." Northeast Bioengineering Conference(NEBEC), 2014 40th Annual. IEEE, 2014.

[22] Dong, Y., K. T. Love, J. R. Dorkin, S. Sirirungruang, Y. Zhang, D. Chen, R. L. Bogorad, et al. 2014. “Lipopeptide Nanoparticles for Potent and Selective SiRNA Delivery in Rodents and Nonhuman Primates.” Proceedings of the National Academy of Sciences 111 (11): 3955–60. doi:10.1073/pnas.1322937111.

[23] Ellesmere OCR. "6.3.1 (a) TLC Interpretation - Ellesmere OCR A Level Chemistry." Google Sites. Ellesmere OCR, n.d. Web. 11 Aug. 2017.

[24]. Zhong, Q., D. Inniss, critical micelle concentration of surfactants in aqueous buffered and unbuffered systems). K. Kjoller, and V. B. Elings. 1993. “Fractured Polymer/Silica Fiber Surface Studied by Tapping Mode Atomic Force Microscopy.” Surface Science 290 (1): L688–92. doi:10.1016/0039-6028(93)90582-5.

[25] Domiguez, Ana et al. “Determination of critical micelle concentration of some surfactants by three tehcniques.” Journal of Chemical Education 74.10 (1997): 1227.

[26] Willhelm, Manfred et al. “’Poly (styrene-ethylene oxide) block

copolymer micelle formation in water: a fluorescence probe study." Macromolecules 24.5 (1991): 1033-1040.

[27] Kalyanasundaram, K., and J.K. Thomas. "Environmental effects on vibronic band intensities in pyrene monomer fluorescence and their application in studies of micellar systems." Journal of the American Chemical Society 99.7 (1977): 2039-2044

[28] Dong, Bin, et al. "Aggregation behavior of long-chain imidazolium ionic liquids in aqueous solution: micellization and characterization of micelle microenvironment." Collids and Surfaces A: Physicochemical and Engineering Aspects 317.1 (2008): 666-672.

[29]. Pecora, R. 2000. "Dynamic Light Scattering Measurement of Nanometer Particles in Liquids." Journal of Nanoparticle Research 2 (2): 123–131.

[30] IDQ. "Dynamic light scattering using silicon avalanche photodiodes." Photosolutions. March 2010. Accessed August 5, 2017: http://www.photonicsolutions.co.uk/upfiles/id100-appnote-dls.pdf

[31] Tscharnuter, Walther. 2000. “Photon Correlation Spectroscopy in Particle Sizing.” Encyclopedia of Analytical Chemistry. http://onlinelibrary.wiley.com/doi/10.1002/9780470027318.a1512/full.

[32] Ray, Gargi Basu, Indranil Chakraborty, and Satya P. Moulik. “Pyrene absorption can be a c onvenient method for porbing ciritcal micellar concentration (cmc) and indexing micellar polarity.” Journal of colloid and interface science 294.1 (2006): 248-254.

[33] The effect of hydrocarbon chain length on the critical micelle concentration of cationic Aguiar, J et al. “On the determination of the critical micelle concentration by the pyrene 1:3 ratio method.” Journal of Colloid and Interface Science 258.1 (2003): 116-122.

[34] Cavalieri, Francesca, Ester Chiessi, and Gaio Paradossi. 2007. “Chaperone-like Activity of Nanoparticles of Hydrophobized Poly(Vinyl Alcohol).” Soft Matter 3 (6): 718. doi:10.1039/b618779j.

[35] Wang, J. “Investigate the effects of molecular structure of lipidoids on self-assembly behaviour” MS Thesis. Tufts University, 2015. February 2017.

[36] Caligur, V. “Detergent Properties and Applications.” Sigma-Aldrich, Sigma-Aldrich, 2008, www.sigmaaldrich.com/technical-documents/articles/biofiles/detergent-properties.html.

[37] Abraham, Sheela A., Dawn N. Waterhouse, Lawrence D. Mayer, Pieter R. Cullis, Thomas D. Madden, and Marcel B. Bally. 2005. “The Liposomal Formulation of Doxorubicin.” Methods in Enzymology, Liposomes, 391 (January): 71–97. doi:10.1016/S0076-6879(05)91004-5.

[38] “Acta Pharmacologica Sinica - Evaluation of Doxorubicin-Loaded PH-Sensitive Polymeric Micelle Release from Tumor Blood Vessels and Anticancer Efficacy Using a Dorsal Skin-Fold Window Chamber Model.” 2017. Accessed August 8. http://www.nature.com/aps/journal/v35/n6/full/aps201412a.html.

[39] Miao, Jing, Yong-Zhong Du, Hong Yuan, Xing-guo Zhang, and Fu-Qiang Hu. 2013. “Drug Resistance Reversal Activity of Anticancer Drug Loaded Solid Lipid Nanoparticles in Multi-Drug Resistant Cancer Cells.” Colloids and Surfaces B: Biointerfaces 110 (October): 74–80. doi:10.1016/j.colsurfb.2013.03.037.

[40] Jin, Zhe-hu, Ming-ji Jin, Chang-gao Jiang, Xue-zhe Yin, Shuai-xing Jin, Xiu-quan Quan, and Zhong-gao Gao. 2014. “Evaluation of

Doxorubicin-Loaded PH-Sensitive Polymeric Micelle Release from Tumor Blood Vessels and Anticancer Efficacy Using a Dorsal Skin-Fold Window Chamber Model." Acta Pharmacologica Sinica 35 (6): 839–45. doi:10.1038/aps.2014.12.

[41] Cuong, Nguyen-Van, Yu-Lun Li, and Ming-Fa Hsieh. 2011. "Targeted Delivery of Doxorubicin to Human Breast Cancers by Folate-Decorated Star-Shaped PEG–PCL Micelle." Journal of Materials Chemistry 22 (3): 1006–20. doi:10.1039/C1JM13588K.

[42] Oliveira, Mariana S., Bhawani Aryasomayajula, Bhushan Pattni, Samuel V. Mussi, Lucas A. M. Ferreira, and Vladmir P. Torchilin. 2016. "Solid Lipid Nanoparticles Co-Loaded with Doxorubicin and α-Tocopherol Succinate Are Effective against Drug-Resistant Cancer Cells in Monolayer and 3-D Spheroid Cancer Cell Models." International Journal of Pharmaceutics 512 (1): 292–300. doi:10.1016/j.ijpharm.2016.08.049.

[43] Yuan, You-Yong, Cheng-Qiong Mao, Xiao-Jiao Du, Jin-Zhi Du, Feng Wang, and Jun Wang. 2012. "Surface Charge Switchable Nanoparticles Based on Zwitterionic Polymer for Enhanced Drug Delivery to Tumor." Advanced Materials 24 (40): 5476–80. doi:10.1002/adma.201202296.

[44] Sipai Altaf Bhai. M*, Vandana Yadav, Mamatha. Y, Prasanth V.V. "Liposomes: An overview. Journal of Pharmaceutical and Scientific Innovation. 1 (1), 2012, 13-21

[45] Zhong, Q., D. Inniss, K. Kjoller, and V. B. Elings. 1993. “Fractured Polymer/Silica Fiber Surface Studied by Tapping Mode Atomic Force Microscopy.” Surface Science 290 (1): L688–92. doi:10.1016/0039-6028(93)90582-5.

[46] Ramana, Lakshmi N., Swaminathan Sethuraman, Udaykumar Ranga, and Uma M. Krishnan. 2010. “Development of a Liposomal Nanodelivery System for Nevirapine.” Journal of Biomedical Science 17 (July): 57. doi:10.1186/1423-0127-17-57.